ISAS - INTERNATIONAL SCHOOL
FOR ADVANCED STUDIES

Domoic Acid Activated Channels in Central Nervous System Neurones

Thesis Submitted for the Degree of
Magister Philosophiae

Candidate:
Xin Zheng

Supervisors:
Prof. Antonio Borsellino
Prof. Oscar Moran

Academic Year 1988/89

TRIESTE

SISSA - SCUOLA
INTERNAZIONALE
SUPERIORE
DI STUDI AVANZATI
TRIESTE
Strada Costiera 11

Domoic Acid Activated Channels in Central Nervous System Neurones

Thesis Submitted for the Degree of
Magister Philosophiae

Candidate:
Xin Zheng

Supervisors:
Prof. Antonio Borsellino
Prof. Oscar Moran

Academic Year 1988/89

This thesis was done
in the
Biophysics Laboratory
of SISSA, Trieste

Content

Chapter 1

Introduction

Nerve cell consists of three functional parts, as shown in Fig. 1.1: dendrites, cell body and axon. The dendrites are a set of branching, tubular cell processes, that extend like antennae from the cell body, and provide an enlarged surface area for the reception of signals from other cells. The

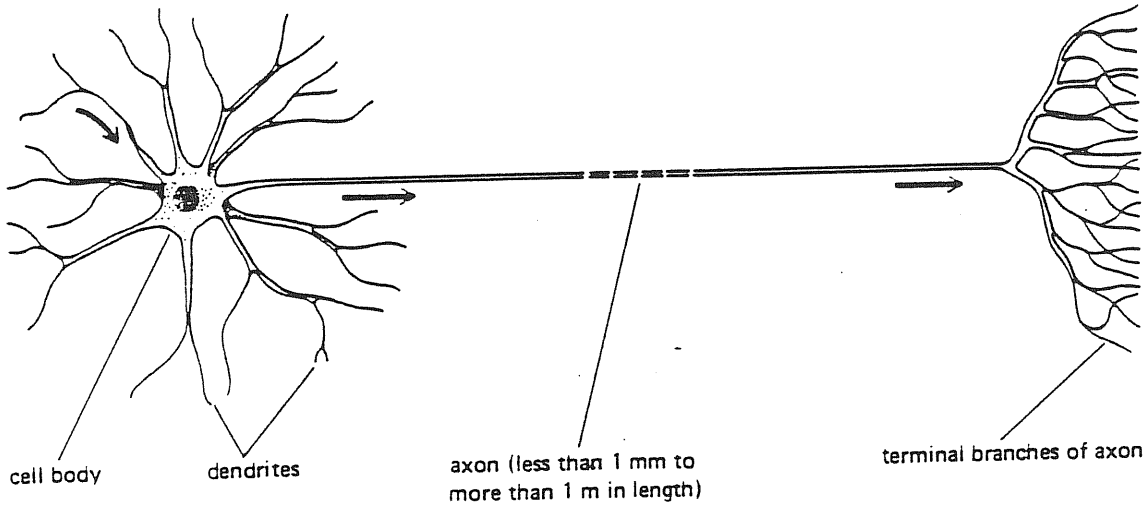

Fig. 1.1 Schematic diagram of a typical neuron of a vertebrate. (From Alberts, *et al.* 1983)

axon is a cell process, generally single and longer than the dendrites, that conducts signals from the cell body to distant targets. It sometimes divides at its far end into many branches, distributing its signals to many destinations (Alberts *et al.* 1983). These nerve fibers can be considered as tubes filled with a watery solution of salts and proteins separated from a different extracellular solution by a relatively impermeable membrane, which is a lipid bilayer. The cell body is also delimited by lipid bilayer and contains the metabolic machinery and the cell nucleous.

There is a voltage difference across the cell plasma membrane, that is called the membrane potential. It is defined as :

$$E_M = E_i - E_o \tag{1.1}$$

where E_M is the membrane potential, E_i and E_o are potentials inside and outside of the membrane respectively. This membrane potential depends on the distribution of electrical charges in both sides of the membrane. Charges are carried back and forth across the nerve cell membrane by small inorganic ions, chiefly Na^+, K^+, Cl^-, and Ca^{2+}, through some selective mechanisms.

The ionic distribution, caused by the selective permeability, should satisfy two basic physical chemistry requirements: the electrical neutrality of both intracellular (except in the proximity of the membrane) and extracellular solutions, and the osmotic balance between the two sides of the membrane. Each individual permeant species of ions is subject to two gradients tending to drive it into or out of the cell——a concentration gradient and an electrical gradient. At equilibrium, there is no net flux for

this species of ions. From Nernst equation (Nernst 1888) the equilibrium potential for this species of ion is :

$$E = \frac{RT}{zF} ln \frac{[N_o]}{[N_i]} \tag{1.2}$$

where R is the gas constant, T is the absolute temperature on the Kelvin scale, z is the valence of ion, F is the Faraday constant, and $[N_o]$ and $[N_i]$ are the concentrations of this kind of ion outside and inside the membrane respectively.

At rest, a special steady-state, the membrane potential take a value, for which the net flow of current across the membrane is zero. The current flowing across the membrane is mainly composed of K^+ current, Na^+ current, and other ionic components, principally Cl^-. These fluxes cross the membranes through channels, carriers and energy driven pumps. From the definition of resting potential, it follows:

$$I_{K^+} + I_{Na^+} + I_{others} = 0 \tag{1.3}$$

Therefore, calling E_K the Nernst equilibrium potential of K^+, E_{Na} the Nernst equilibrium potential of Na^+ and E_{other} the equilibrium potential of other mechanism, Eq(1.3) can be expressed by:

$$g_K(E_{rest} - E_K) + g_{Na}(E_{rest} - E_{Na}) + g_{other}(E_{rest} - E_{other}) = 0 \tag{1.4}$$

From the beginning of this century, it is known that excitable cell

membranes are far more permeable to K^+ ions than to other ions at rest (Hille 1984, Bernstein 1902,1912). In other words, g_K is relatively large. Therefore resting potential, E_{rest}, must be close to potassium equilibrium potential E_K. Otherwise K^+ current should be too large and could not be balanced by other currents. In reality, the concentration of Na^+ is about ten times lower inside the cell than it is outside, while the distribution of K^+ is roughly the reverse. So, from the Nernst equation at room temperature the resting potential, which is, in fact, very near to the potassium equilibrium potential, is between -70 to -100 mV (Alberts, *et al.* 1983). If the membrane potential differs from this resting potential, a net current will flow, tending to return the membrane potential to the resting potential. When the membrane potential is raised from resting potential toward zero, i.e., the inside becomes less negative with respect to outside, the membrane is said to be depolarized. When the procedure is opposite, the membrane is said to be hyperpolarized.

Transport of small charged molecules (ions) across the lipid bilayer of the membrane is achieved by specialized transmembrane proteins, each of which is responsible for the transfer of a specific molecule or group of closely related molecules. Some membrane transport proteins, called channels, form aqueous pores which permit ions to move across the lipid bilayer by a process called passive transport, that can occur spontaneously under the driving of electrochemical gradient. Others, called carriers, bind the specific molecule to be transported and translocate it across the membrane. Some carriers function as pumps that actively drive the movement of ions against their electrochemical gradient by so called active transport, which must be tightly coupled to a source of metabolic energy. This mechanism

guarantees the existence of electrochemical gradients. A schematic diagram of membrane transport proteins is shown in Fig. 1.2.

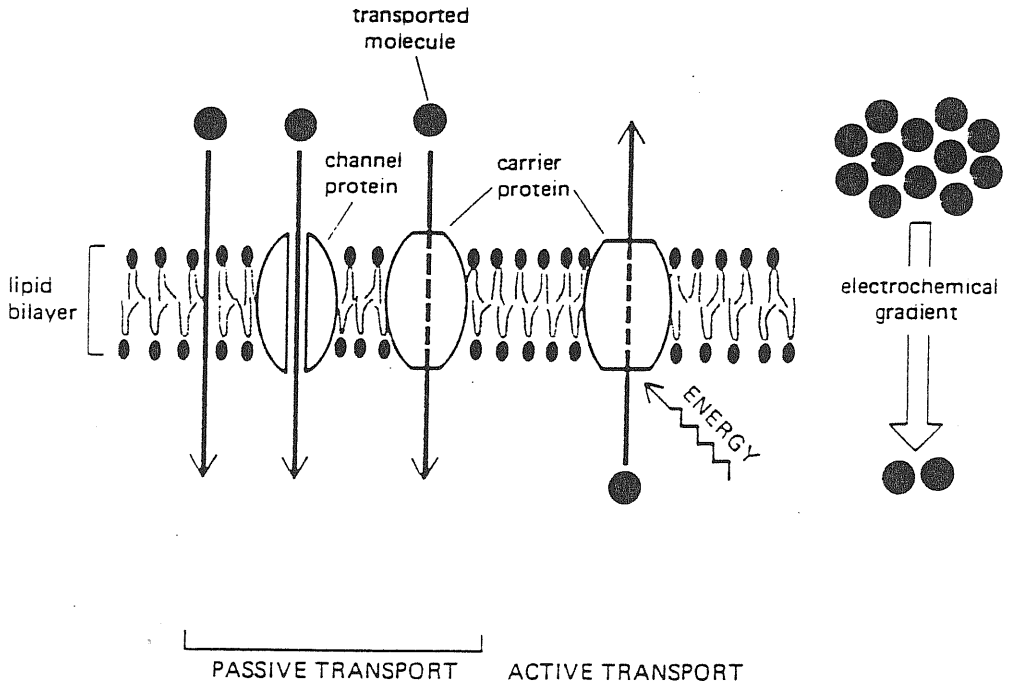

Fig. 1.2 Schematic diagram of membrane transport proteins. (From Alberts *et al.*,1983)

Channels are formed by proteins, some of them are open for most of the time, others open only transiently. The former channels are said to be leak channels while the latter are said to be "gated" channels. Gated channels can be divided into two major groups. Some of them open in response to an extracellular ligand binding to a specific cell-surface receptor and are called ligand-gated channels, which play a central role in the operation of chemical synapses (see later: Synapsis and Synaptic Transmission) others open in response to a change in the membrane potential and are called

voltage-gated channels; there are also a small part of channels which open in response to changes in the intracellular concentration of specific ions or mechanical stimuli. Fig. 1.3 shows the schematic diagrams of ligand-gated and voltage-gated channels. Each voltage-gated channel has a selectivity filter, which permits specific ions, such as Na^+, K^+, Ca^{2+}, Cl^- pass through it and the channel is named correspondingly as voltage-gated Na^+ channel, voltage-gated K^+ channel, and so on. Voltage-gated channels——especially voltage-gated sodium channels——play the key role in the electrical activity by which action potentials are propagated along a nerve cell process.

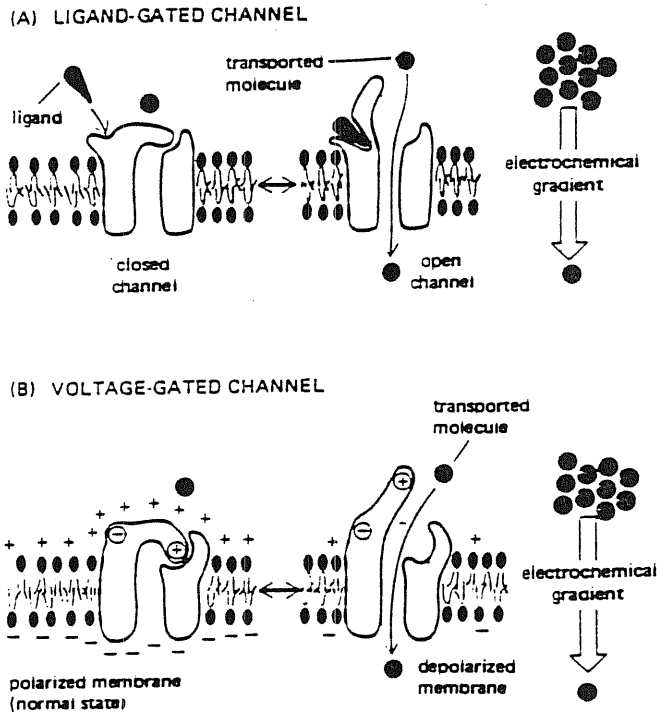

Fig. 1.3 Schematic diagram of ligand-gated and voltage-gated channels. (From Alberts *et al.* 1983)

Action Potential

It is possible to depolarize an axon by injecting current through a microelectrode inserted into it. If the current is small, the polarization will be subthreshold. In this case no channels will open as a response to the membrane potential change. In the resulting steady state, the inflow of current through the microelectrode will be balanced by an outflow of current across the membrane in the neighborhood of the microelectrode. If the cell processes are considered as a core-conductor models— a thin tube of membrane that is filled with electrically conducting fluid (axoplasm) and immersed in another electrically conducting medium (extracellular fluid), cable-theory can be used to treat their distribution of current and potential (Lakshminarayan 1984). Cable equation can be expressed as:

$$V + r_m C_m \frac{\partial V}{\partial t} = \frac{r_m}{r_i} \frac{\partial^2 V}{\partial x^2} \tag{1.5}$$

where $V = E_M - E_{rest}$ is the electrotonic potential, $r_m = R_m/2\pi a$ is the resistance across a unit length of the surface of passive membrane(Ω cm), R_m is the resistance of unit area of membrane(Ω cm^2), a is the radius of cable cylinder(cm), C_m is the capacitance per unit area of membrane (F cm^{-2}), $r_i = R_i/\pi a^2$ is the core resistance per unit length(Ω cm^{-1}), R_i is the specific resistivity of the intracellular medium(Ω cm), t is the time and x is the spatial coordinate taken along the cable.

Substituting for $r_m C_m (= \tau_m)$ and $r_m/r_i (= \lambda^2)$, cable equation can be written as:

$$\lambda^2 \frac{\partial^2 V}{\partial x^2} - V - \tau_m \frac{\partial V}{\partial t} = 0 \tag{1.6}$$

τ_m and λ are called time constant and space constant respectively. In steady state, V depends on x but not on t, and so $\partial V/\partial t = 0$, the cable equation reduces to:

$$\lambda^2 \frac{\partial^2 V}{\partial x^2} - V = 0 \tag{1.7}$$

For the boundary conditions that $V = V_0$ at $x = 0$, the solution of this equation is $V = V_0 exp(-x/\lambda)$. The consequence of this pattern of current flow is that the magnitude of a disturbance of the membrane potential falls off exponentially with the distance from the source of the disturbance. This is a passive spread of electrical signal along a nerve cell process.

When the inflow of current is large enough so that the membrane is depolarized above a critical potential level, the threshold, the nerve impulse or action potential, will be initiated. At the threshold, the voltage-gated Na^+ channels open, allowing Na^+ ions to flow into the cell, thus this patch of membrane is depolarized further and causes the other Na^+ channels located on neighboring patches to open as well. This process continues rapidly in a self-amplifying fashion until the membrane potential has shifted from its resting value (≈ -70 mV) to the Na^+ equilibrium potential ($\approx +50$ mV). At this point, the net electrochemical driving force for the flow of Na^+ channels is zero and a new resting state, with all Na^+ channel permanently open, is established. However, this new resting state is not stable. The automatic inactivation process leads the Na^+ channels to close

gradually and remain closed until the membrane potential has returned to its initial negative resting value. In many types of neurons, this recovery is hastened by the presence of voltage-gated K^+ channels in the plasma membrane. Like the Na^+ channels, these K^+ channels open in response to membrane depolarization, but they do so relatively slowly. By increasing the permeability of the membrane to K^+ just as the Na^+ channels are closing through inactivation, the K^+ channels help to bring the membrane rapidly back toward the K^+ equilibrium potential, so returning it to the resting state.

The signals used by neurons to transmit information are membrane potential changes caused by electrical current flowing across their membranes. Only two types of signals, localized potentials and action potentials, as mentioned above, can be carried by neurons. Localized potentials take place at special regions, such as sensory nerve endings and synapses. They grade continuously in size and can only spread a short distance ($1 \sim 2$ mm) through a passive process. During this short distance transmission their magnitudes are severely reduced and time courses are distorted. The localized potential enables individual cells to perform their integrative function and to initiate nerve impulse. Action potential is an all-or-none signal, which travels rapidly without distortion from one end of the nerve to another. It transmits nerve impulses caused by localized potential.

A very important characteristics is that when the membrane is depolarized beyond the threshold, action potential will be initiated automatically and bears no relation to the amplitude and time duration of the original stimulus. The differences between localized potential and action potential are illustrated clearly by Fig. 1.4.

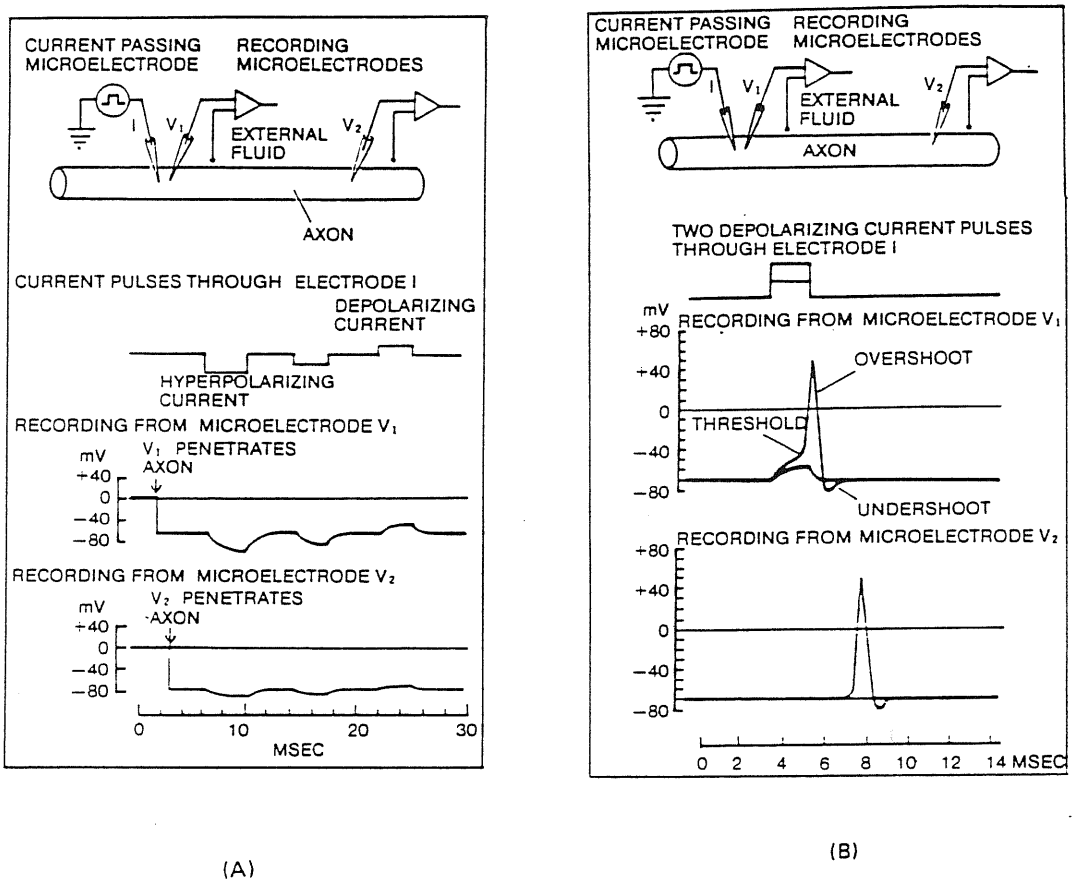

Fig. 1.4 Intracellular recording from a large axon with microelectrodes. I is used to pass pulse of current that produces localized potentials. V_1 and V_2 are used to measure membrane potential at different points. (A) Localized potential. Through I input two hyperpolarizing pulses and one depolarizing pulse. Depolarizing current under the threshold. V_1 next to I, V_2 is placed about 1mm away from V_1. (B) Action potential. Input a depolarizing current over membrane threshold. V_1 next to I, V_2 is 2cm away V_1. (From Kuffler, *et al.*, 1984)

Synapsis and Synaptic Transmission

Synapses are the junctions between nerve cells where they transfer signals. The typical structure of synapsis is shown in Fig. 1.5.

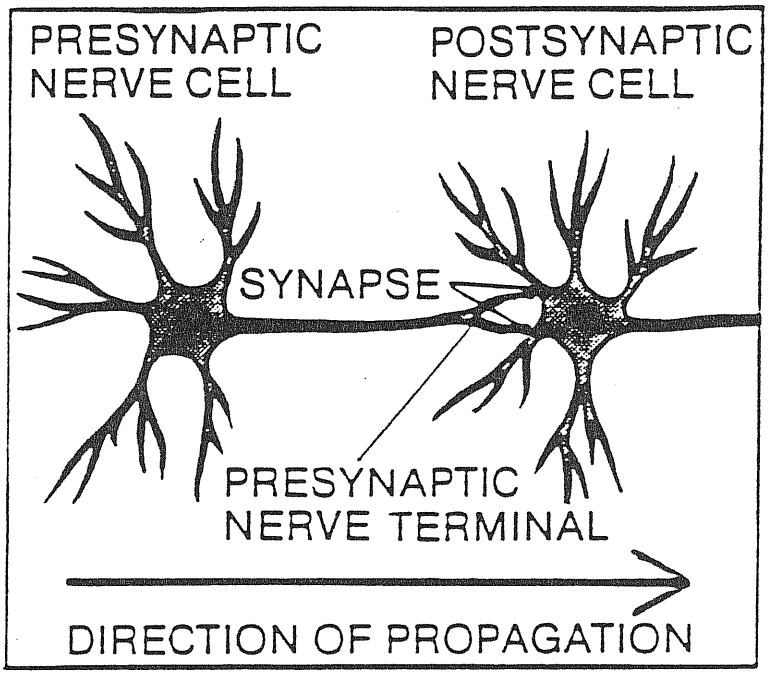

Fig. 1.5 The junction between cells is called Synapsis.
(From Kuffler *et al.*, 1984)

Neurons influence each other by two ways: excitation, by which one cell tends to produce impulses in other ones, and inhibition by which one cell tends to prevent impulses from arising in other cells. The mechanism of excitation is depolarization of the postsynaptic membrane and that of inhibition is the hyperpolarization of the postsynaptic cell's membrane. A

cell receives many excitatory and inhibitory inputs from other cells and in turn supplies many others. For example, a nerve cell can accommodate as many as 200,000 synapses (Kuffler, *et al.* 1984). The final behaviour, excited or inhibited, is determined by an integrative process whereby a cell adds together all the incoming signals. The transfers of signals taking place at synapses are called synaptic transmission. Two distinct modes, one electrical and the other one chemical, are used to produce synaptic transmission. The electrical synapses are the sites where two nerve cells make a low-resistance electrical contact. The electrical currents generated by an impulse in the presynaptic nerve terminal can spread directly into the next neuron through these low-resistance pathways, which are called gap junctions (Kuffler, *et al.* 1984). Chemical synapses, the most common transmission mechanism, being graphically shown in Fig. 1.6, appear as well-defined structures (Langley and Anderson 1892, Loewi 1921, Dale 1953). The presynaptic terminals contain numerous vesicles close to the membrane. Clefts that are filled with extracellular fluid separate the membranes of the two cells. Electrondense material is often seen in the cleft and on the two membranes.

When the action potential arrives at the presynaptic terminal, it opens the voltage-gated Ca^{2+} channels, allowing Ca^{2+} to enter the axon terminal. The influx of calcium, although small, has important effects. It raises the free-Ca^{2+} concentration in the presynaptic terminal and then causes the vesicles to fuse with the presynaptic membrane, discharging their contents——neurotransmitter ——into the synaptic cleft. The gated influx of Ca^{2+} into the axon terminal is essential to synaptic transmission. In low-calcium medium the release of neurotransmitter can be reduced or com-

pletely eliminated, but injection of Ca^{2+} into cytoplasm at axon terminal can lead to the release of transmitter even without electrical stimulation of the axon (del Castillo and Stark 1952, Douglas 1978, Alberts, *et al.* 1983).

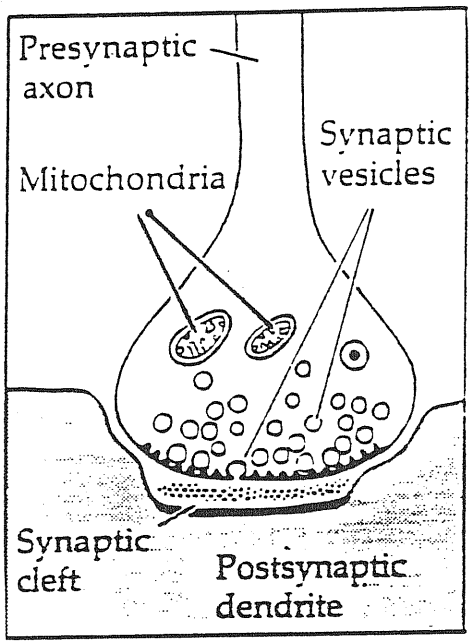

Fig. 1.6 The structure of chemical synapsis
(From Kuffler,*et al.* 1984)

When the neurotransmitter diffuses across the synaptic cleft and arrives at postsynaptic membrane, it will act on the postsynaptic cell by binding to receptor proteins in the postsynaptic membrane whereby this chemical signal will be converted to electrical signal again. The conversion is achieved by ligand-gated ion channels in postsynaptic membrane. When the neurotransmitter binds to these channels externally, some times it directly

changes their conformation—-opening to let ions cross the membrane—-and thereby alter the membrane potential. Some times it leads to the generation of a intracellular signal involving second messengers, which in turn activates protein kinases that can phosphorylate ion channels and thus alter the cell's electrical behaviour. Unlike the voltage-gated channels responsible for action potentials and for transmitter release, the ligand-gated channels are relatively insensitive to the membrane potential. They can not by themselves produce an all-or-none self-amplifying excitation. Instead, they produce an electrical change that is graded according to the intensity and duration of the external chemical signal——that is, according to how much transmitter is released into synaptic cleft and how long it remain there. Greatly prolonged exposure to neurotransmitter can cause the channel to enter a desensitized state.

Postsynaptic ligand-gated channels have two other important properties. First, the receptors associated with them have an enzyme-like specificity for particular ligands so that they respond only to one neurotransmitter, the one released from the presynaptic terminal or its chemically related substances; other substances are virtually without effects. Second, different types of channels are characterized by different ion selectivities: some may be selectively permeable to Na^+, others to K^+, others to Cl^-, and so on, while others may, for example, be relatively unselective among the cations but exclude anions. When the postsynaptic ligand-gated channel is selectively permeable to the cations which will flow into the cell, the neurotransmitter causes a depolarization of the postsynaptic membrane, therefore the synapsis mediates a excitatory effect. If the postsynaptic ion channel is selectively permeable to anions or some cations, such as K^+,

which will flow out of the cell, and the membrane will be hyperpolarized, the synapsis is an inhibitory synapsis.

There are two major groups of neurotransmitters: one group is formed by the neuropeptides and another group by the small molecules, such as acetylcholine and certain monoamines and amino acids (Alberts, *et al.* 1983).

Excitatory Amino Acids

The dicarboxylic amino acids L-glutamate and L-aspartate were the first compounds examined for an action on mammalian central nervous system (CNS) neurons, using the technique of microiontophoresis, in conjunction with extracellular recording from interneurons and Renshaw cells, and intracellular recording from motoneurons in the spinal cord of anesthetized cat (Curtis, *et al.* 1959, 1960, Mayer and Westbrook 1987). The excitatory actions of L-aspartate and L-glutamate were found to be of similar potency and due to membrane potential depolarization, with a consequent reduction in threshold for the initiation of action potentials evoked by excitatory synaptic potential or depolarizing electrotonic potentials. A similar excitatory action of L-glutamate and L-aspartate and their analogues was also observed by using extracellular recording in experiments on neurons in the cerebral cortex and cerebellar cortex (Mayer and Westbrook 1987, Krnjević and Phillis 1963).

The first studies by Curtis and his colleagues (1960) explored only the actions of glutamate, aspartate, and cysteate; but the fact that many other acidic amino acids have similar effects soon became apparent (Curtis and

Watkins 1960, McLennan 1987), and some were considerably more potent than the naturally occurring compounds (Curtis and Watkins 1963). All of these acidic amino acids are called excitatory amino acids (EAA). Some examples of these potentially valuable unphysiological excitatory amino acids are N-methyl-D-aspartic acid (NMDA), Kainic acid (Shinozaki and Konishi 1970, Shinozaki 1978), Quisqualic acid (Shinozaki and Shibuya 1974, Shinozaki 1978), and Domoic acid (Shinozaki and Shibuya 1976). These compounds, most of them, are natural products, are related structurally to glutamate, and share with them both neuroexcitatory and neurotoxic properties (McGeer, *et al.* 1978). The structure of the above excitatory amino acids is shown in Fig. 1.7. The essential substituents on the molecule which conferred activity were stated to be the presence of an amino group optimally situated α to a carboxyl group and spaced two or three carbon atoms distant from a second acidic site (Curtis and Watkins 1960).

There is considerable evidence that glutamate is a principal neurotransmitter that mediates fast excitatory synaptic transmission in the vertebrate CNS (Curtis and Johnston 1974, Krnjević 1974, Watkins and Evans 1981, McLennan 1981, di Chiara and Gessa 1981, Foster and Fagg 1984, Iversen 1984, Cull-Candy and Ogden 1986). The development of selective pharmacological agents has allowed the electrophysiological characterization of neuronal receptors for this excitatory amino acid. These studies have identified three major classes of excitatory amino acid receptors based on, and after named by, the agonists preferred by the receptor (Watkins and Evans 1981, Hampson and Wenthold 1988): N-methyl-D-aspartate (NMDA), Quisqualate, and Kainate (KA) receptors (Jahr and Stevens 1987, Shinozaki 1988, Usowicz, *et al.* 1989). The concept of

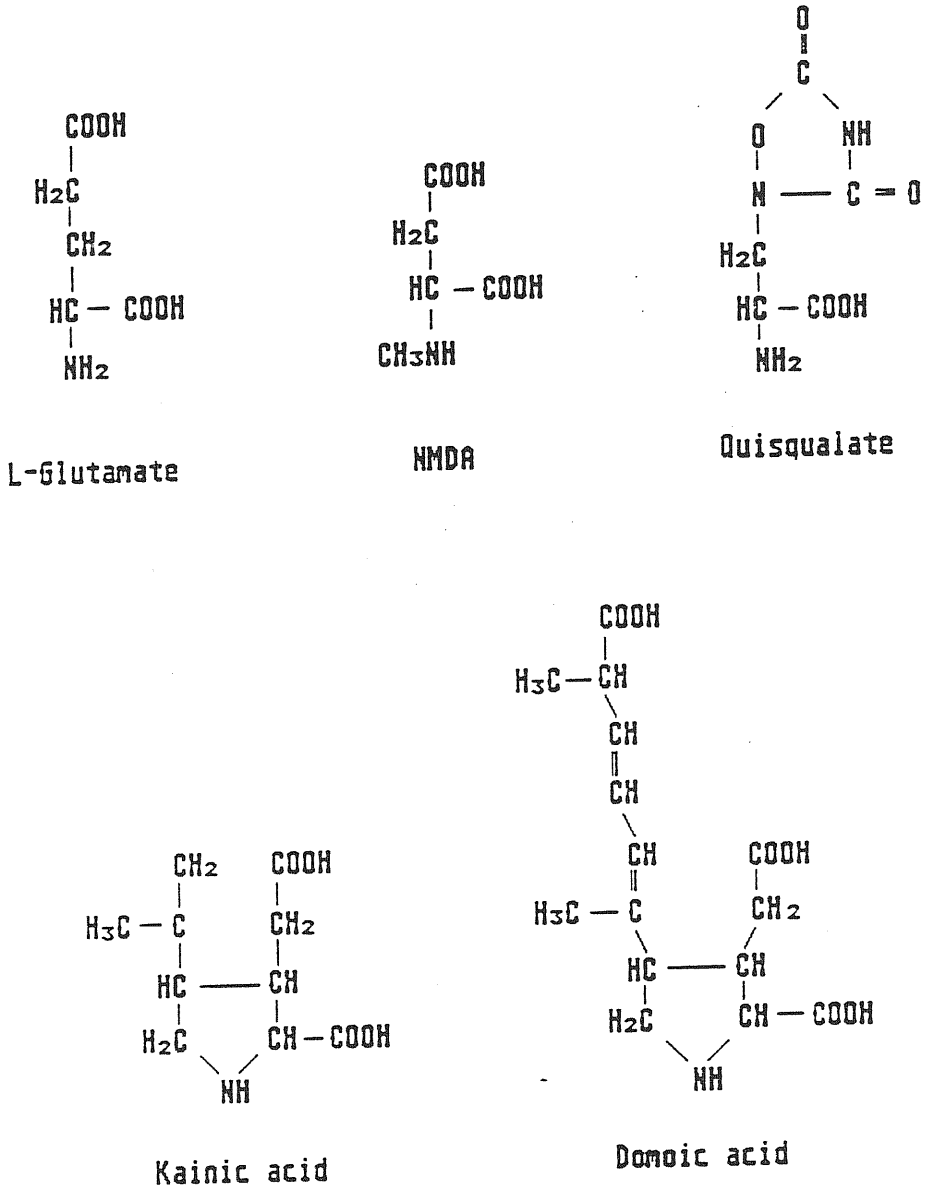

Fig. 1.7 Structures of L-glutamate, NMDA, quisqualic acid, kainic acid and domoic acid

separate receptor subtypes activated preferentially by L-glutamate and L-aspartate developed from observations suggesting a differential sensitivity of some mammalian spinal neurons to these amino acids (Duggan, 1974), and the finding that this differential sensitivity was even greater when NMDA and KA were used to excite spinal neurons (Johnston *et al.*, 1974, McCulloch *et al.*, 1974). With the observation that Mg^{2+} acts to selectively block responses to NMDA but not KA or quisqualate (Davies and Watkins 1977, Evans *et al.*, 1977), the concept of separate Mg^{2+} sensitive (NMDA) and Mg^{2+} insensitive (non-NMDA) excitatory amino acid receptor subtypes evolved.

Recently some researchers focus their attention on domoic elicited current in mammalian CNS neurones for two reasons. Domoic acid can be used as a tool to study glutamate receptor subtypes. As Fig. 1.7 shows, domoic acid is structurally related to kainic acid. It is one of the compounds which has a high affinity for the KA receptors (Slevin *et al.*, 1983, Hampson and Wenthold 1988). The compounds were tested on rat spinal interneurons by microelectrophoresis (Biscoe, *et al.* 1972) and on frog spinal motoneurons by superfusion of the procaine-blocked (Biscoe *et al.*, 1975) hemisected spinal cord *in vitro*. On both of these preparations the anions of domoic acid were found to be at least two orders of magnitude more potent than L-glutamate, and equal to or stronger than kainate (Biscoe *et al.*, 1975). For these reasons, domoic acid is an effective agonist in the study of kainate receptors.

Another interesting characteristics of domoic acid is its toxicity. Domoic acid is produced by several species of phytoplankton and is taken by marine bivalves, as mussels, either directly from water or indirectly from

their food. Normally it will not exist in human's CNS, but erroneous ingestion of domoic acid will poison human central nervous system. In late November/early December 1987, more than one hundred people were hospitalized after eating mussels from a certain location on Prince Edward Island, Canada. In older people, the symptoms tended to be neurological and loss of memory was encountered in a number of cases. The toxin was later identified by the National Research Council of Canada, Halifax Research Laboratory, as domoic acid. The excitatory amino acid toxicity depends on the opening of some kinds of ionic channels.

Granule Cells of the cerebellum

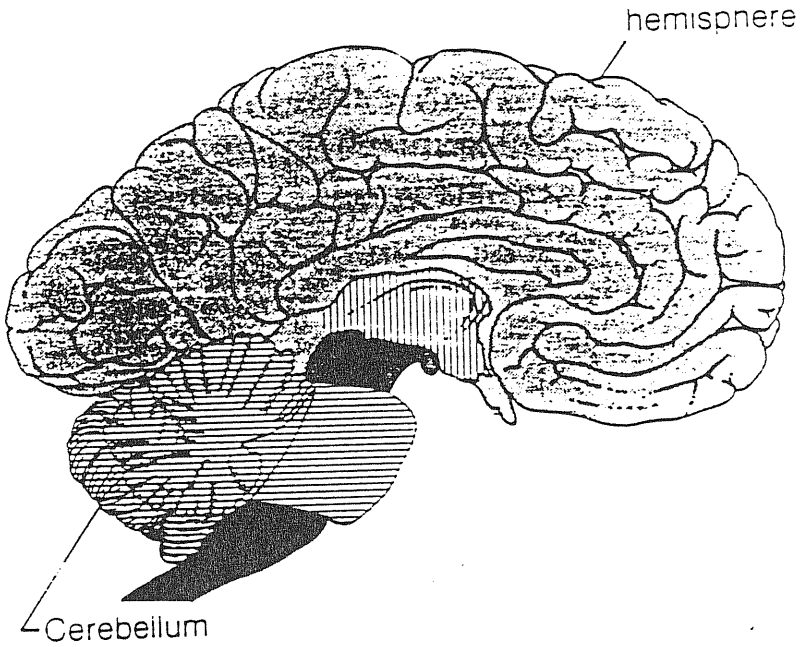

Fig. 1.8 cerebellum (From Kolb and Whishaw 1980)

Cerebellum was probably the first part specialized for sensory-motor coordination. The precise function of cerebellum varies from one part of the structure to another, depending on the connections with the rest of the nervous system. Parts that receive most of their impulses from the vestibular system help to maintain the body's equilibrium, whereas parts receiving impulses mainly from the body senses are involved with postural reflexes and coordinating functionally related muscles. The major part of the cerebellum receives impulses from the neocortex and functions primarily to promote the efficiency of skilled movements (Kolb and Whishaw 1980).

Cerebellum has over 10^{10} cells, but only five different kinds of neuronal types. These five different kinds of neurons are Purkinje cell, Golgi cell, basket cell, granule cell and stellate cell (Kuffler *et al.*, 1984). Among them the number of granule cells approximates to 10^{10} to 10^{11} (Braitenberg and Atwood 1958). The cell bodies of different kinds of cells are confined to distinct layers as it is shown in Fig. 1.9. The input to the cerebellum comes from different sources, as various sensory structures in muscle, skin, and joints, from visual and auditory cortex. All the information is handled by repeated groupings——granule cells, basket cells, stellate cells and Golgi cells. All of these cells directly or indirectly act upon the Purkinje cells which provide the only output from the cerebellar cortex (Kuffler *et al.* 1984)

Granule cells are the main component of the granular layer of the mammalian cerebellar cortex. They can accept the messages from the axons of peripheral nervous system and transfer the messages through their axons, which traverse and make connections with the Purkinje cell processes in the molecular layer.

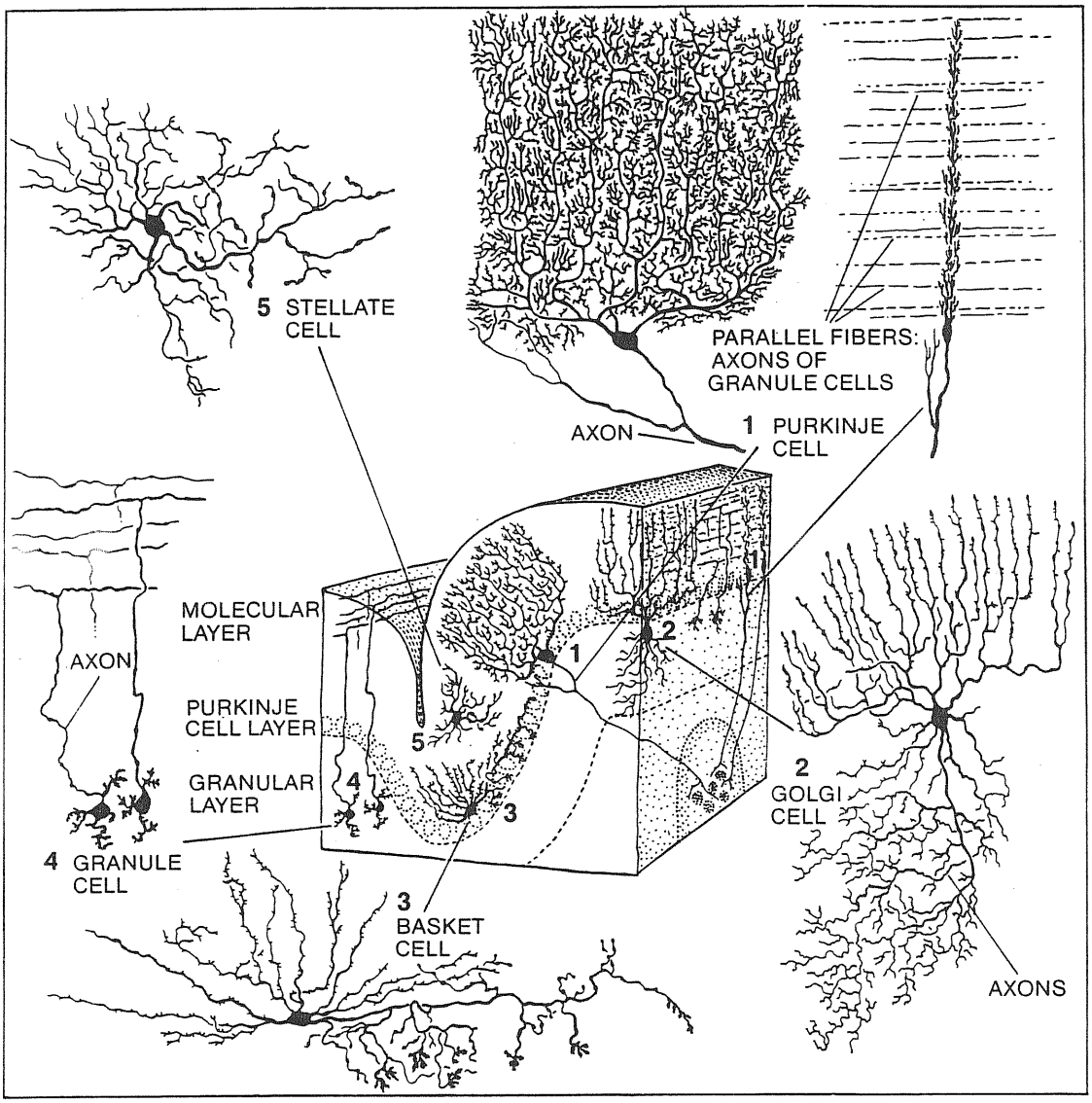

Fig. 1.9 Positions of different neurons in cerebellum(From Kuffler *et al.*,1984)

Fig. 1.9 Positions of different neurons in cerebellum(From Kuffler *et al.*,1984)

Cerebellar granule cells consist of one ideal system to study the EAA receptor-channel complex in central neuron primary cultures. Some of the reasons that prompted us to use the granule cells to study domoic acid activated channels are: Rat cerebellar granule cells grown in "high" potassium medium (25 mM) consist in a homogeneous and long-term cell cultures (Gallo *et al.*, 1982). Granule cells receive synapses from mossy fibers. These synapses are glutamatergic, that implies that granule cells have glutamic acid (and related agonist) receptors (for example see Gallo *et al.*, 1982, Kohler and Schwarcz 1983, Cull-Candy *et al.*, 1988). On the other hand, the neurocytochemical and morphological characteristics of the granule cells (Gallo *et al.*, 1982 Hockberger *et al.*, 1987), as well as some biochemical characteristics related with the possibility of the relations between the glutamate receptor and second messengers activated metabolic pathways (for example see Novelli *et al.*, 1988) have been studied. Finally, some experiences on the electrophysiology of the granule cells have been acquired in our laboratory. These experiences are related to the study of NMDA-receptors (Sciancalepore and Moran 1989) and voltage dependent ionic channels (Borsellino *et al.*, 1988, Lin 1988, Lin and Moran 1989).

Chapter 2

Material and Method

Domoic acid activated channels on cultured cerebellar granule cells have been studied. Voltage-clamp technique, both cell-attach and outside-out configurations, was used in experiments.

Cell culture

Primary cultured cerebellar granule cells were prepared from 8-day-old neonatal rats by the following updated procedure based on the previously described method (Novelli, *et al.* 1988, Sayan 1987). Cerebella were removed under sterile conditions from rats pups and were placed in solution 1 (see table 2.1). The meninges and the blood vessels were peeled off carefully of the removed cerebella and then preliminary minced the cerebella on a chopping surface with sterile razor.

The minced tissue were suspended in solution 1 and centrifuged at speed 1000 RPM for 1 minute. The cell pellet was resuspended in trypsin containing solution 2 (see table 2.2). The suspension was shaken for 10 minutes at 37°C. During this procedure, the trypsin in solution 2 digested the connective tissue. After digestion, solution 3 (see table 2.3), containing trypsin inhibitor and DNase was added into the suspension. The suspension

was recentrifuged at 1000 RPM for 1 minute and then the cell pellet should underwent a mechanical separation—— sucking up and releasing down in a fire polished Pasteur pipette in solution 4 (see table 2.4). After this separation solution 5 (see table 2.5) was added to the suspension and re-centrifuged at 1000 RPM for 5 minutes. The cell pellet was resuspended in culture medium (see table 2.6) and diluted to 0.75 million cells per milliliter.

An appropriate volume ($\sim$ 2 ml) of cell suspension was added to each 35 mm Petri dish, which has been pre-covered by poly-L-lysine (5μg/ml), in order to obtain a cell density of 1.5 million per dish. The plated neurons were placed into a 37° C, 5% CO_2, maximum humidity incubator (Heraeus). 10 μM Cytosine Arabinoside Furanoside (Sigma, ST. Louis,U.S.A.) as mitotic inhibitor was added in each dish after about 19 hours *in vitro* to inhibit the growth of non-neuronal cells. In this way, the culture is $\sim$ 90% glutamatergic granule cells and the window for use of the neurons is about two weeks after start of incubation.

Solutions for Electrophysiology

The extracellular and intracellular solutions used in electrophysiology experiments were listed in table 2.7 and 2.8. 128 mM Cs^+ and 10 mM tetraethylammonium (TEA) were used in intracellular and extracellular solution respectively for blocking the voltage-gated potassium channels. 1 μM tetrodotoxin (TTX, Sigma) was added in extracellular solution for blocking voltage-gated sodium channels.

Table 2.1 Solution 1

Composition	Concentration	Comments
NaCl	124.00mM	(1) pH=7.4, adjusted with NaOH.
KCl	5.37mM	(2) similar with physiological
NaH_2PO_4	1.01mM	solution.
D-glucose	14.50mM	(3) to be used for washing
HEPES	25mM	cerebellar tissue.
Phenol red	27μM	
$MgSO_4$	1.2mM	
BSA*	3mg/ml	

*bovine serum albumin (Sigma, St Louis)

Table 2.2 Solution 2

Composition	Concentration	Comments
NaCl	124.00mM	(1) made of 50ml solution 1
KCl	5.37mM	+ 12.5mg trypsin.
NaH_2PO_4	1.01mM	(2) for digesting the connective
D-glucose	14.50mM	tissue.
HEPES	25mM	
Phenol red	27μM	
$MgSO_4$	1.2mM	
BSA	3mg/ml	
trypsin*	0.25mg/ml	

* Sigma

Table 2.3 Solution 3

Composition	Concentration	Comments
NaCl	124.00mM	(1) made of 17ml solution 1 +
KCl	5.37mM	8ml solution 4.
NaH_2PO_4	1.01mM	(2) for stopping trypsinization
D-glucose	14.50mM	and degradation DNA.
HEPES	25mM	
Phenol red	27μM	
$MgSO_4$	1.7mM	
BSA	3mg/ml	
DNase*	25.6μg/ml	
SBTI**	166.4μg/ml	

* Sigma

** soybean trypsin inhibitor (Sigma)

Table 2.4 Solution 4

Composition	Concentration	Comments
NaCl	124.00mM	(1) made of 15ml solution 1
KCl	5.37mM	+ 1.2mg DNase + 7.8mg
NaH_2PO_4	1.01mM	SBTI + 150μl $MgSO_4$
D-glucose	14.50mM	stock solution (155mM).
HEPES	25mM	
Phenol red	27μM	(2) for proceeding mechanical
$MgSO_4$	2.75mM	separation.
BSA	3mg/ml	
DNase	80μg/ml	
SBTI	0.52mg/ml	

Table 2.5 Solution 5

Composition	Concentration	Comments
NaCl	124.00mM	(1) made of 12.5ml solution 1 +
KCl	5.37mM	15μl $CaCl_2$ stock solution
NaH_2PO_4	1.01mM	(81.6 mM) + 100μl $MgSO_4$
D-glucose	14.50mM	stock solution(155mM).
HEPES	25mM	
Phenol red	27μM	(2) Add Ca^{2+},which can not
$MgSO_4$	2.44mM	be added before the operation
$CaCl_2$	0.1mM	of trypsin.

Table 2.6 Neuron Growth Solution

Composition	Quantity	Comments
BEM*	500ml	for neuron growth.
L-glutamine	147mg	
KCl	825mg	
gentamicin**	1ml×50mg/ml	
FCS***	50ml	

* basal Eagle's medium (Flow Laboratories,Scotland, Irvine)

** Sigma

*** fetal calf serum heat inactivated (Flow Laboratories)

Domoic acid used in experiments was obtained from Diagnostic Chemicals Limited, Canada. All other chemical substances used were obtained from Prolabo (Paris, France) or Sigma.

Table 2.7 Extracellular Solution

Composition	Concentration	Comments
KCl	3mM	pH=7.4 adjusted with NaOH
$CaCl_2 \cdot 2H_2O$	1.5mM	
NaCl	125mM	
TEA	10mM	
HEPES	10mM	
glucose	9.5mM	

Table 2.8 Intracellular Solution

Composition	Concentration	Comments
CsCl	128mM	pH=7.4 adjusted with KOH
EGTA	10mM	
HEPES	10mM	
glucose	9mM	

Electrophysiology

Voltage clamp experiments offer several advantages over membrane potential recording for studying the action of neurotransmitter substances, principally because many conductance mechanisms show a nonlinear voltage dependence, and it is easier to record and analyse such events if the membrane potential is under experimental control. Under optimal conditions, the technique also allows measurement of the rate constants controlling the opening and closing of ion channels.

Voltage Clamp

A steady membrane potential is maintained when there is no net loss or accumulation of charge in the cell——that is, if current is injected into a cell through a microelectrode the current flowing through the membrane channels is exactly equal and opposite to the current injected. Therefore, if the membrane potential is kept constant, the current flowing through the membrane channels can be deduced from the current through the current electrode. Based on this simple idea, the voltage clamp technique was developed (Cole 1949, Marmont 1949). Traditional voltage clamp technique requires the use of two microelectrodes to insert into a cell; one for recording membrane potential, and one serves for injecting current to control the membrane potential. A suitable electronic circuit is used to adjust the injected current automatically according to the signal from the voltage-measure electrode. This holds the membrane potential steady at any designated voltage, which is called command voltage. By setting different command voltages and measuring the injected current that is required to maintain them, one can systematically investigate the membrane con-

ductance as a function of the membrane potential.

Patch clamp

Now patch clamp technique is widely used. In 1976, Neher and Sakmann (1976) introduced a method, extracellular patch clamp, for recording the current in a small patch of membrane under voltage-clamp conditions. This patch clamp technique has allowed, for the first time, the currents in single channel to be observed. In 1981, the patch clamp technique was improved by Hamill *et al.* (1981) to allow a higher resolution current recording. In this technique a small heat-polished glass pipette is pressed against the membrane, forming a electrical seal with a resistance of the order of 50 MΩ. When precautions are taken to keep the pipette surface clean and when the suction is applied to the pipette interior, tight pipette-seals with resistances of $10 \sim 100$ GΩ can be obtained. The high resistance of this seal ensures that most of the currents origination in a small patch of membrane flows into the pipette, and from there into current-measurement circuitry. The high resistance is also important because it reduces the level of background noise in the recording and increases the resolution. Gigaohm seal is not only electrically tight, but also mechanically very stable. Following withdrawal from the cell membrane a membrane vesicle forms occluding the pipette tip (Hamill and Sakmann 1981, Neher 1981, Hamill, *et al.* 1981). The vesicle can be partly disrupted without destroying the giga-seal, leaving a cell-free membrane patch that spans the opening of the pipette tip in either outside-out or inside-out configurations. This allows single channel current recordings from isolated membrane patches in defined media, as well as solution changes during the measurements (Horn and Patlak 1980, Hamill and Sakmann 1981, Hamill *et al.* 1981). The pipette can also

be kept in cell-attached state before or after the disrupting of the membrane vesicle to form cell-attached configuration or whole cell recording configuration respectively. The procedures which lead to various recording configurations are shown in Fig. 2.1. In this thesis, both cell-attached and outside-out configurations were used.

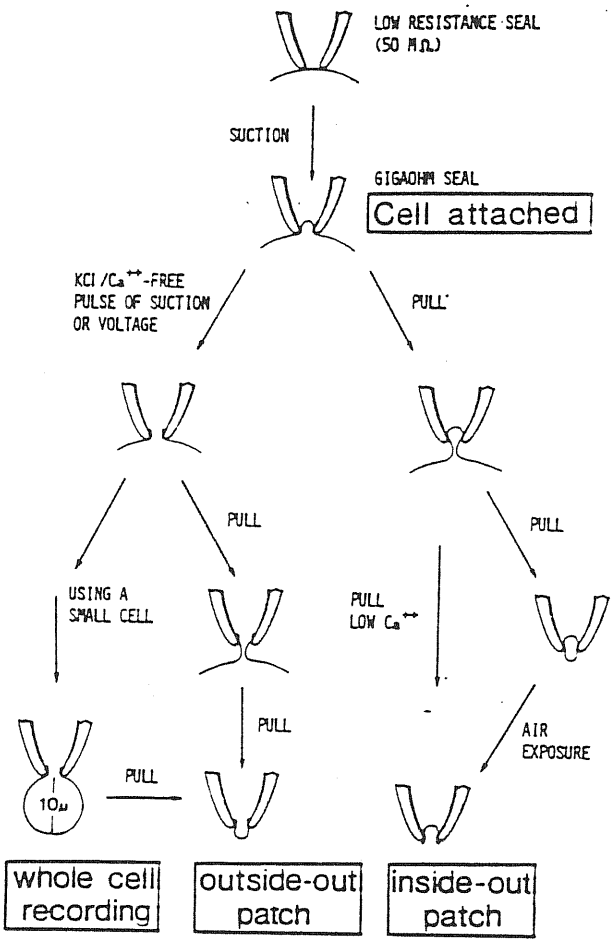

Fig. 2.1 Schematic representation of the procedures which lead to different recording configurations (From Hamill *et al.*, 1981)

Pipette Fabrication

Patch pipette were pulled from Borosilicate-glass capillaries (Hilgenberg, West Germany) with filament inside. The parameters of capillaries are: length=80 mm, interdiameter =1.05 mm, outerdiameter=1.50 mm. The capillaries were pulled in two steps in a L/M-3P-A patch pipette puller (List-Electronic, Eberstadt, West Germany).

The pipettes were coated with Sylgard (Dow Corning, Seneffe, Belgium) under a Steni SV8 low magnification microscope (Zeiss, West Germany) no more than one hour before using. Heat polishing was performed under a 320× magnification Standard 16 microscope (Zeiss) after coating Sylgard. A pipette with resistance $\sim$ 10 MΩ (after polishing) can be obtained by this process (measured with experimental solutions).

Background Noise and Circuit

Usually the signals from ionic channels are small both in magnitude and in time duration. To detect these signals, it is necessary to reduce the background noise to as low as possible.

The background noise which limits the resolution of recording consists of four contributions: membrane, membrane pipette combination, pipette and recording electronics, see Fig. 2.2.

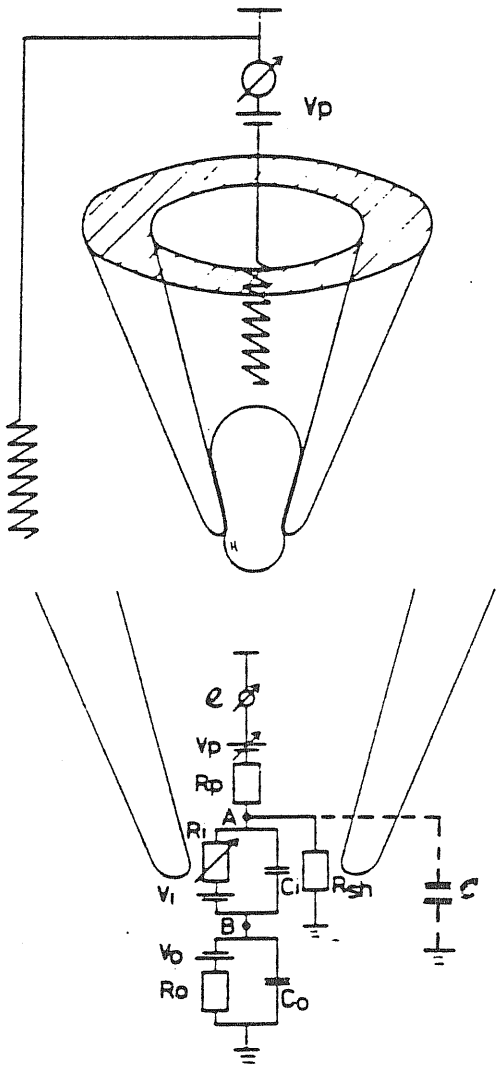

Fig.2.2, The major noise source in patch clamp experiment. (from Hamill *et al.* 1981).

Two halves of the vesicle are represented by RC combinations in series. R_i, R_0 and C_i, C_0 are the membrane resistance and capacitance. V_i, V_o are the electromotive forces of the two halves of the vesicle. R_p is the access resistance of the unsealed pipette. V_p is the electrode potential. R_{sh} is the shunt resistance which includes the seal resistance and the glass wall resistance (reciprocal of bulk conductance). C is the capacitance of the thin film of solution that creeps up the outer wall of the pipette. e is the noise source from the recording circuit.

Apart from the noise sources in the instrumentation, there are inherent limits due to the conductances of the patch membrane and the seal. One noise source is the Johnson noise of the membrane seal combination, which has a one-side current spectral density:

$$S_I(f) = 4KTRe[Y(f)] \tag{2.1}$$

where K is Boltzman constant, T is absolute temperature and $Re[Y(f)]$ is the real part of the admittance. The membrane-pipette seal can be modelled as a simple parallel RC circuit. So

$$Y(f) = \frac{1}{R} + i2\pi fC \tag{2.2}$$

and

$$Re[Y(f)] = \frac{1}{R} \tag{2.3}$$

therefore

$$S_I(f) = \frac{4KT}{R} \tag{2.4}$$

which decreases with the increasing of the seal resistance. Another noise source is the "shot noise" expected from ions crossing the membrane, for example, through leakage channel or pumps. The spectral density can be roughly estimated as (Steven 1972, Läuger 1975):

$$S_I = 2Iq \tag{2.5}$$

where q is the effective charge of the current carrier and I is the unidirectional current.

The pipettes used for our experiments also have some intrinsic noise. Three main sources of Johnson noise in pipettes were aware: first, most serious noise arises from a thin film of solution that creeps up the outer wall of the pipettes; second, the bulk conductivity of the pipettes glass introduces a significant noise; and final, the pipettes access resistance R_{acc} and the capacitance of the tip of the pipettes C_{tip} constitute a noise source. Each of them can be modelled by a series RC circuit with the admittance:

$$Y(f) = \frac{(2\pi fC)^2 R + i2\pi fC}{1 + (2\pi fCR)^2} \tag{2.6}$$

So from (2.1) it follows:

$$S_I(f) = 4KT\frac{(2\pi fRC)^2}{R[1+(2\pi fRC)^2]} \tag{2.7}$$

The noise from the thin film of solution can be reduced considerably by Sylgard coating applied to the pipettes: the hydrophobic surface of Sylgard prevents the formation of a solution film and the thickness of the coating reduces the capacitance C. Choosing hard electrode glass, as borosilicate glass, can reduce the noise arising from bulk conducting of electrode glass. The R_{acc} and C_{tip} introduced noise can be reduced in pipettes having steeper tapers near the tip, reducing R_{acc}, or having the coating extended closer to the tip, reducing C_{tip}.

The last noise source is the recording electronics. The instrument used for experiments is EPC-7 external patch clamp amplifier (List-Electronic, West Germany). It is essentially made of two functional parts: the I-V converter, which will directly connect with the pipette holder; and the EPC-7 controller which contains the signal amplifier together with other specific functional elements, as filters and capacity transient and series resistance compensation. Its recording electronics is diagramed simply in Fig.2.3.

The high-value resistor $R_f(\leq 10\text{G}\Omega$) in the I-V converter introduces the predominant Johnson noise. When $R_f \leq 10\text{G}\Omega$, C_f has no contribution to noise, i.e. $Re[Y(f)]$ has no frequency dependence. However when R_f above $10\text{G}\Omega$, there is a more complicate RC combination and it is difficult to correct this frequency response. The operational amplifier in I-V converter is another main noise source at high frequency region. This noise is imposed by the feed-back loop on the pipette and the input of the amplifier, causing a current to charge C_p and C_{in}. The resulting current

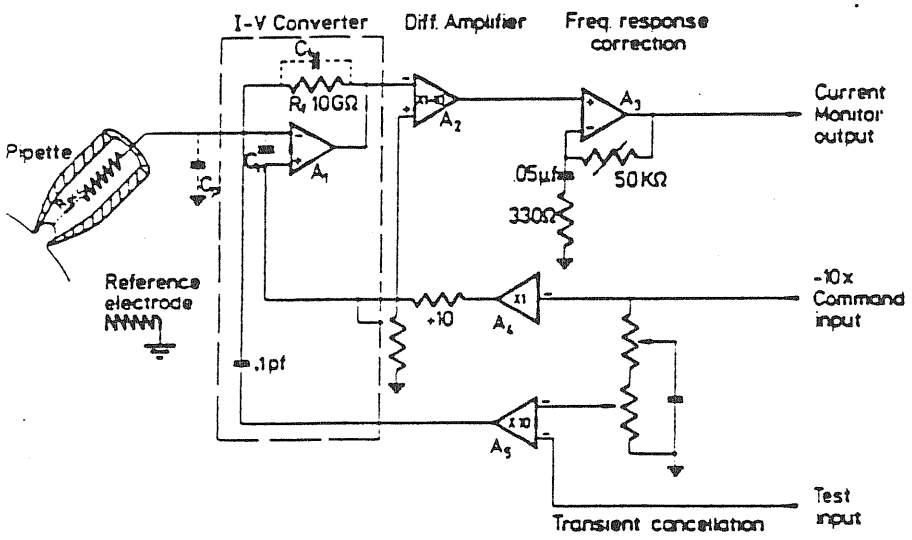

Fig. 2.3 A simplified diagram of EPC-7 recording system.
(from Hamill *et al.* 1981)

fluctuation has the spectrum:

$$S_I(f) = [2\pi f(C_p + C_{in})]^2 S_{V(A)}(f) \tag{2.8}$$

where $S_{V(A)}(f)$ is the amplifier voltage noise spectral density. Using short pipette and low level solution in combination with avoiding unnecessary shielding of the pipette and holder will be helpful for minimizing C_p, therefore reduce $S_I(f)$. At lower frequency, amplifier introduced noise can be neglected.

The transient cancellation circuit (see Fig.2.3) was designed to reduce the capacitors charging current which is 4-5 orders of magnitude larger than typical signal current, caused by a step change in the pipette potential.

Recording

The recording instruments used in experiments were organized as in Fig. 2.4. The $I - V$ converter of EPC-7 was mounted on a three-dimensional CP-198 micromanipulator (Physik Instrumentes). The pipette was manipulated under a 320× magnification IM35 microscope (Zeiss).

The signals through the pipette were first amplified by the $I - V$ converter of EPC-7 and then sent to EPC-7 controller. One output of EPC-7 controller was filtered by a built in 10kHz 3-pole Bessel filter and fed to the data recorder, which is a combination of a modified PCM device (Digital Audio Processor, PCM-501ES, Sony, Japan) and video tape recorder (Super β Stereo Video Cassette Recorder, Sony). The other output of EPC-7 was filtered at 315 Hz bandwidth by a 4 poles Bessel filter (Ithaco 4302, USA)

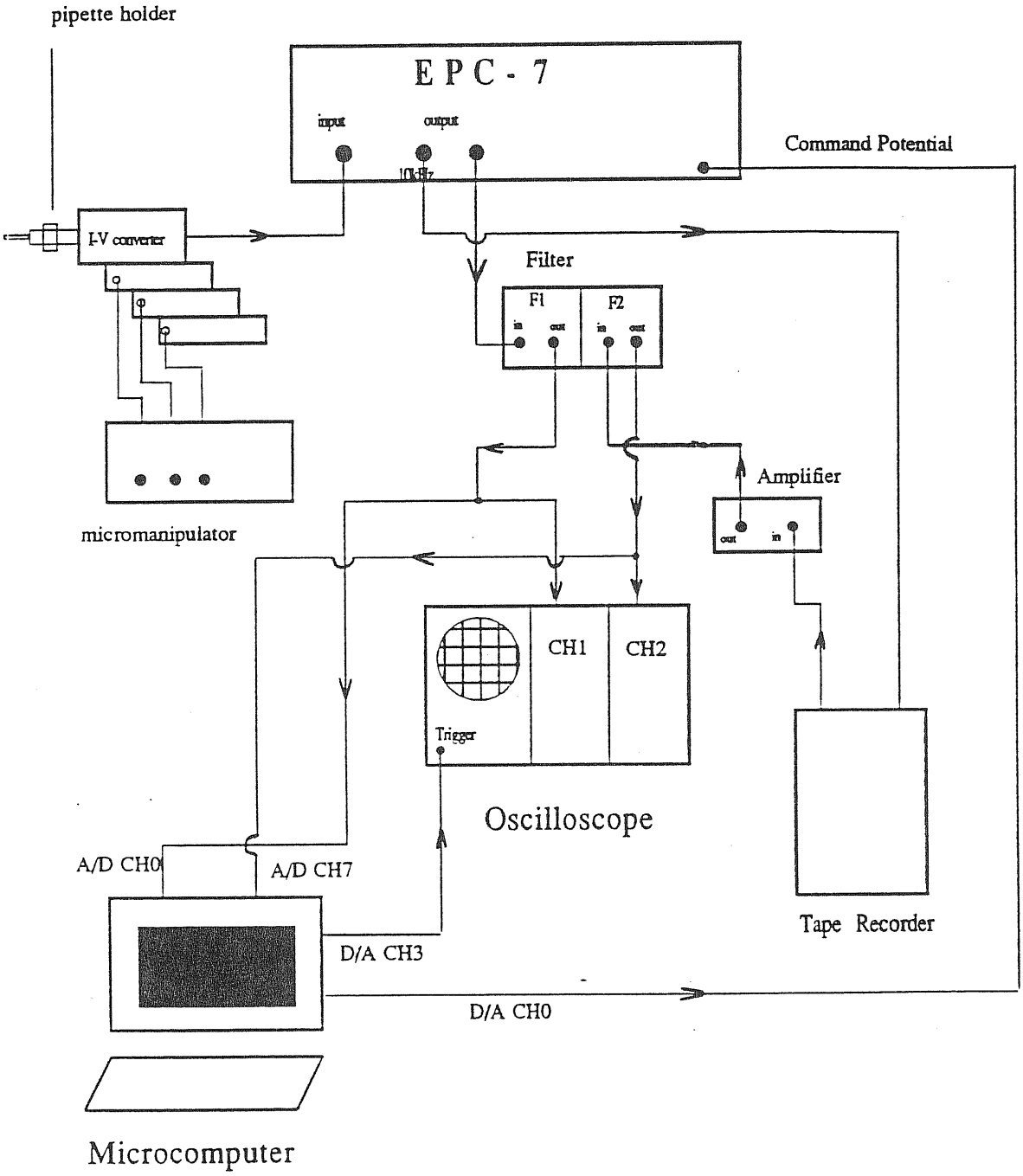

Fig 2.4 The diagram of the recording equipment network.

and sent to both a storage oscilloscope (Tektronix 5111A) for monitor, and a A/D and D/A converter (Max-Planck Institut für biophysikalische Chemie designed, Instrutek version) which connected to a microcomputer (Atari 1040ST). The microcomputer was used to control the experiments and all the data analyses.

Analysis

The recorded signals in the video cassette were amplified by a linear amplifier constructed in the laboratory and filtered at a cut-off frequency 1kHz by a 4 poles Bessel filter (Ithaco 4302). The signal was digitalized by the A/D converter and transferred to the microcomputer. The acquisition was performed by the Recorder program, written in Modula–2 by H.Affolter of Yale University. According to the sampling theorem (Shannon and Weaver 1964), the Nyquist frequency f_c, which determined by sampling interval Δ as:

$$f_c = \frac{1}{2\Delta} \tag{2.9}$$

should be larger than the upper frequency limitation of signal, usually five times of the limitation. Since our upper frequency limitation was 1kHz, the sampling frequency was chosen as: $f_c \geq$ 5kHz, and the sampling interval should be:

$$\Delta = \frac{1}{2f_c} \leq \frac{1}{2 \times 1(kHz)} = 0.5(ms) \tag{2.10}$$

In our analysis the sampling interval was 0.2 ms.The acquired data files

from the Recorder program were analysed by TAC threshold analysis program, which descended from the program THAC described by Colquhoun and Sigworth (1983) and written by Affolter and Sigworth, to get current amplitude and the distributions of dwell times.

The histogram which displays the distributions of dwell times was plotted in square-root ordinate with a logarithmic time axis (Sigworth and Sine,1987). If the distribution consists of a sum of m exponential components, the probability density function (pdf) takes the form:

$$f(x) = \sum_{j=1}^{m} a_j f_g(x - s_j) \tag{2.11}$$

where $s_j = ln(\tau_j)$ is the logarithm of the jth time constant, a_j is the fraction of the total events represented by that component, x is the logarithm axis arising from the transformation $x = ln(t)$, and $f_g(x - s_j)$ is the "generic" pdf defined as:

$$f_g(z) = exp[z - exp(z)] \tag{2.12}$$

Maximum likelihood method was used to fit the above distributions. The likelihood is equal to the probability of obtaining a particular set of observed dwell-times t_j, given the form of distribution and the parameters Θ, and is proportional to the product over the N observations.

$$Lik = \prod_{j=1}^{N} f(t_j|\Theta) \tag{2.13}$$

where $f(t_i|\Theta)$ is the probability density function evaluated at t_j with the particular set of parameters Θ. For a sum of m exponential components:

$$f(t_j \mid \Theta) = \sum_{i=1}^{m} \frac{a_i}{\tau_i} exp(t_j/\tau_i) \tag{2.14}$$

where Θ consists of the entire set of the coefficients a_i and time constants τ_i. Since

$$\sum_{i=1}^{m} a_i = 1$$

the set of parameters Θ has $2m - 1$ independent elements.

In practice the log likelihood is used with the correction of the absence of very short and very long intervals that are due to the experimental limitations. The log likelihood with correction is given by (Colquhoun and Sigworth, 1983):

$$L(\Theta) = \sum_{j=1}^{N} ln[f(t_j|\Theta)/p(t_{min}, t_{max}|\Theta)] \tag{2.15}$$

where $p(t_{min}, t_{max} \mid \Theta)$ is the probability that dwell-times fall within the range of experimentally measurable times characterized by t_{min} and t_{max}. The fitting of experimental sets of dwell-time measurements with maximum likelihood method is typically done by maximizing the logarithm of the likelihood with respect to the set of fitting parameters Θ, i.e. finding the set of parameters Θ that maximizes $L(\Theta)$.

The channel conductance can be obtained by using the TAC program to get the current amplitude and dividing this current by its corresponding

membrane potential. To reduce the errors produced by calculating the conductance only under one membrane potential, we measured the channel current at a set of different potentials and calculated the conductance by evaluating the slope of the I-V relation.

Chapter 3

Results

Electric responses from domoic acid activated channels were observed in rats cerebellar granule cells using the patch clamp technique. The currents were measured under different potentials using two different patch clamp configurations: outside-out and cell-attached.

In outside-out configuration recordings, 62% (15 in 24 patches) of patches were discarded because of their presence of spontaneous fluctuations. One example of the recordings being of spontaneous fluctuations is shown in Fig. 3.1. Among the remained 38% (9 in 24 patches) patches, the probability of finding domoic activated channels was 44% (4 in 9 patches).

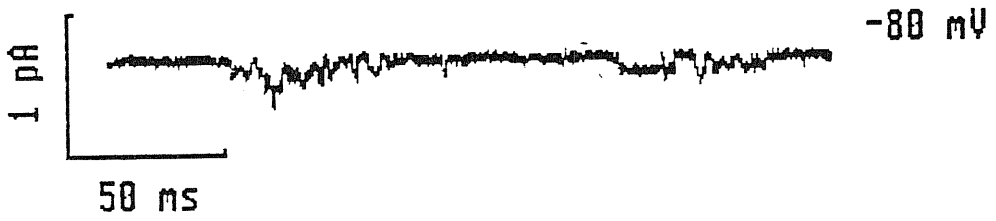

Fig. 3.1 Spontaneous fluctuations in outside-out patches. Obtained from granule cells of 5 days *in vitro*. Temperature was 24°C. Membrane potential was −80 mV. Bandwidth was 1 kHz.

Some experiments were done in cell-attached configuration. Five of them were recorded without domoic acid in the pipettes solution as control, while fourteen patches with 10 μM domoic acid in the pipettes solution. Among the latter 43% (6 in 14 patches) of the patches were observed to have domoic activated channels.

The statistics of finding domoic activated channels in this two groups of experiments were coincident with each other quite well. It seems we can induce that the probability to find domoic activated channels in granule cells is around 50% if the pipettes have the unsealed resistance around 10 MΩ. In this time the tip opening area of the pipettes is about 5 μm^2 according to empirical experiences (Sakmann and Neher 1983).

The density of domoic acid activated channels can be roughly estimated on the bases of above results. We know, if the tip opening area of the pipettes is about 5 μm^2, we can "catch" the channel in every two patches on the average. In practice, the area of the membrane patches is larger than the pipettes opening area. If we suppose the membrane vesicle is a half sphere, the area of the patch should be two times of that of its cross section. Therefore, we can roughly say every patch has a area about 10 μm^2. Thus empirically we can estimate that the density of domoic acid activated channels is about 0.05 μm^{-2}.

$I - V$ relation and reversal potential

In outside-out configurations, the domoic induced currents were measured under standard condition: monovalent cations concentration of bath solution (125 mM Na^+, 3 mM K^+) and that of the solution in pipettes

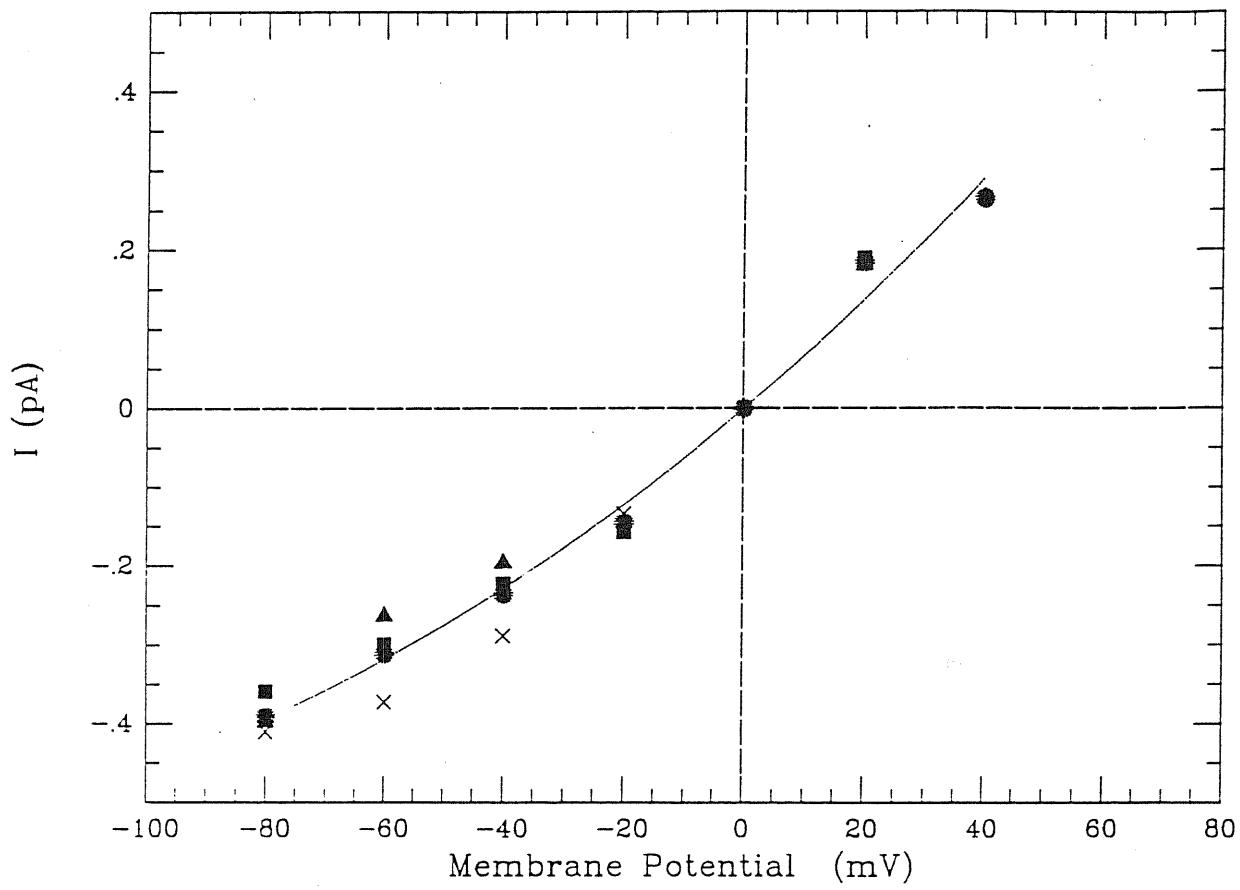

Fig. 3.2 $I - V$ relations obtained from granule cells in outside-out patches. Triangles, squares, crosses and stars in the figure are used to label the values from different experiments. Each of them was obtained by the average of at least 30 current amplitudes. The experimental values show the presence of the outward rectifications.

(128 mM Cs^+) are equal. The $I - V$ relation was obtained by measuring the current amplitudes at various membrane potentials. $I - V$ relations under standard condition were given in Fig. 3.2. $I - V$ relation shows a slight outward rectification and indicates that the domoic elicited currents reversal potential under standard condition is 0 mV.

Conductances

A series of domoic elicited current, recorded in outside-out configuration in the membrane potential range from −80 mV to 40 mV are shown in Fig. 3.3 and 3.4. After the patches had been made, the control trace was first recorded for at least 3 minutes before beginning the neurotransmitter perfusion in order to control the stability of the patches and to assess the absence of other ionic channels. Then, 10 μM domoic acid was applied directly in the extracellular solution.

Since the $I - V$ relations are not linear, the conductance are different at different membrane potentials. Fig. 3.2 shows the tendency of increasing of conductance with the increasing of the membrane potential. However, as we already seen in Fig. 3.2, this conductance changing is not significant. The ratio of the domoic-induced current at 40 mV to that at −40 mV was about 1.1.

In outside-out configuration, 4 experiments gave the similar results. Fig. 3.5 shows the amplitude histogram obtained at −80mV membrane potential. The amplitude histogram shows very clear that there are two event peaks, one locates at 0.19 pA and the other locates at 0.39 pA. They result from the subconductance and the main conductance respectively.

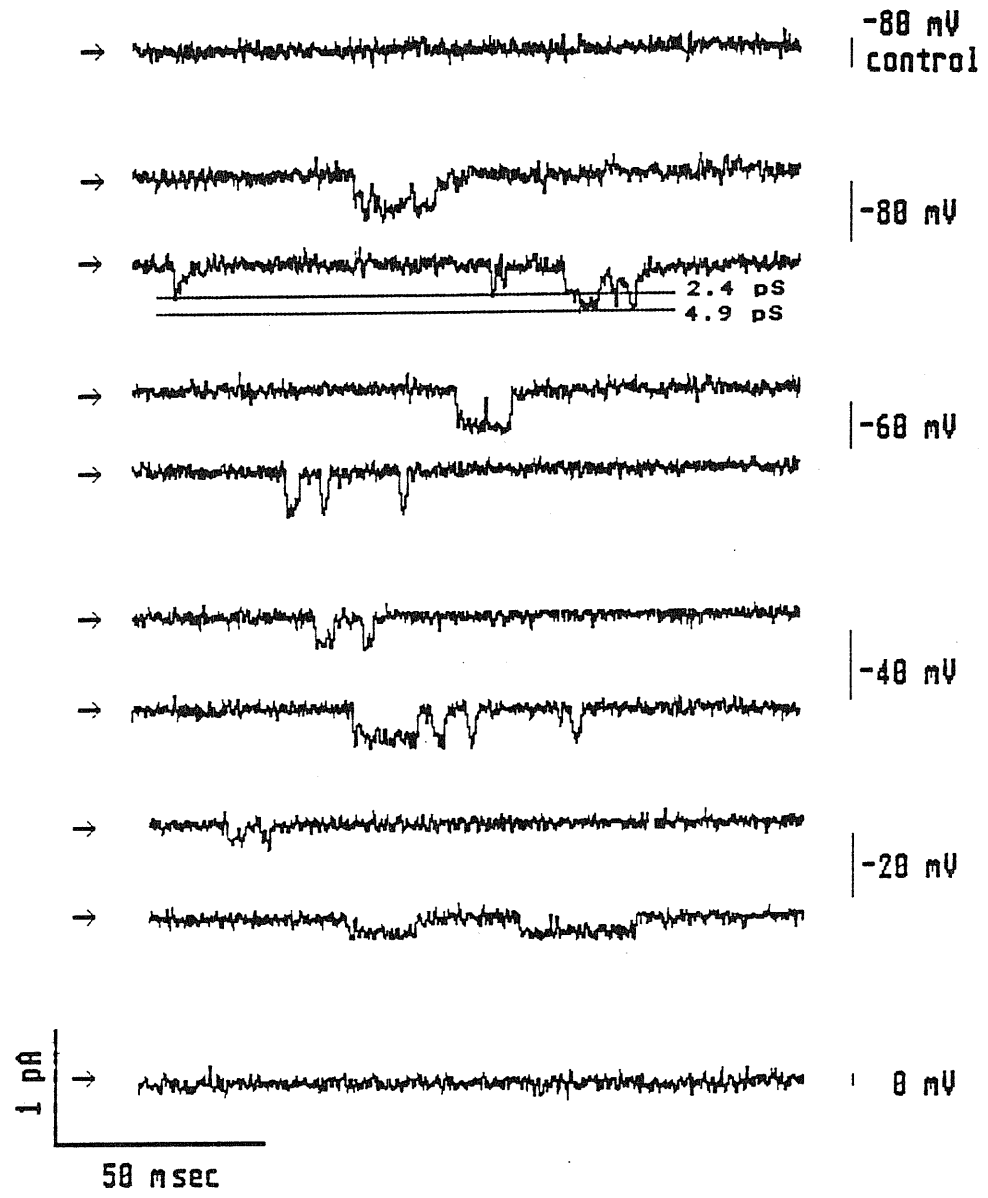

Fig. 3.3 Domoic elicited currents with the main conductance about 4 pS in outside-out patches. Obtained from granule cells of 5 days *in vitro*. Temperature was 24°C. Membrane potential varied from −80 mV to 0 mV. Bandwidth was 1 kHz. 10 μM domoic acid was applied in bath solution. The upper trace is the control recorded before domoic acid perfusion. Some subconductance can be observed in graph.

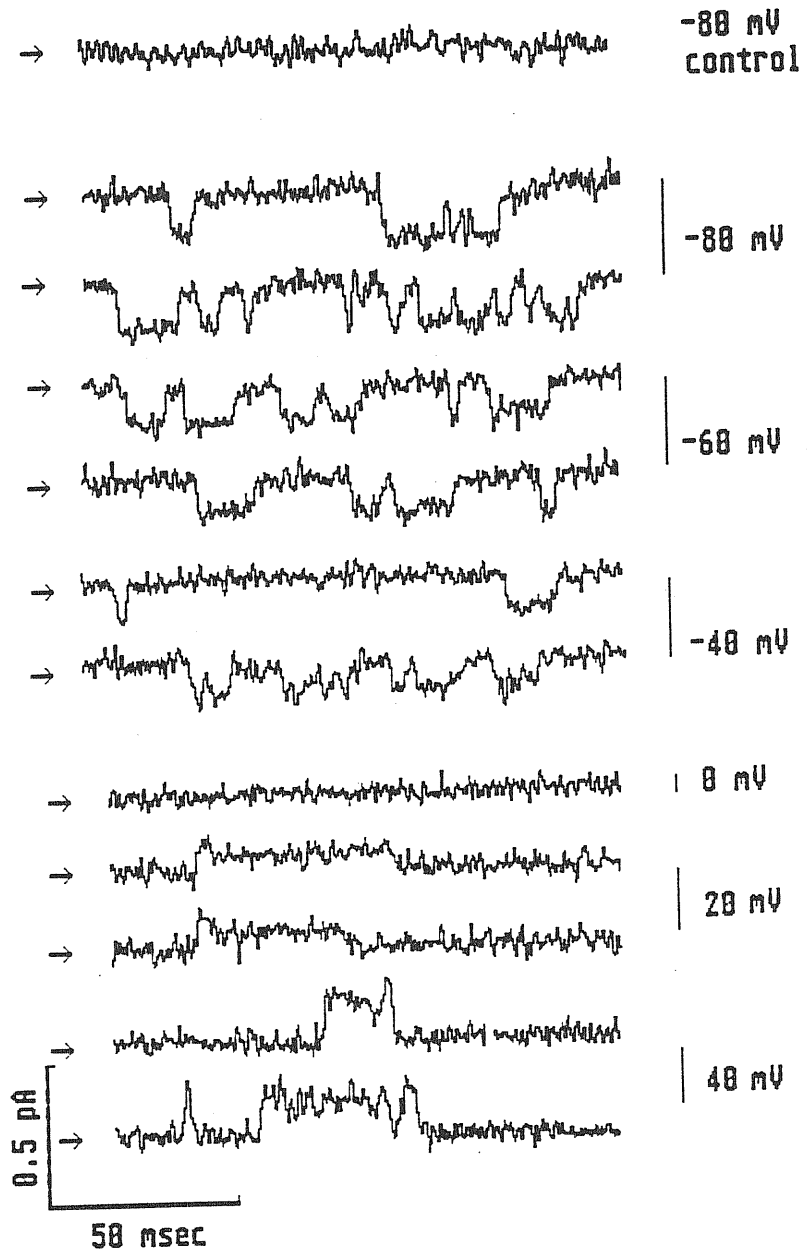

Fig. 3.4 Domoic elicited currents with the main conductance about 4 pS in outside-out patches. Obtained from granule cells of 8 days *in vitro*. Temperature was 24°C. Membrane potential varied from −80 mV to 40 mV. Bandwidth was 500 kHz. 10 μM domoic acid was applied in bath solution. The upper trace is the control recorded before domoic acid perfusion.

The result shows that the main conductance is 4.91±0.23 pS (mean ± S.D.). This main conductance was also obtained from cell-attached experiments when the electrode potential changed from 60 mV to −40 mV. Since the resting potential of granule cells in primary culture is around −70 mV (Borsellino *et al.*, 1988), above potential range corresponds to a membrane potential range from −130 mV to −30 mV. Four experiments gave a similar value as: 4.4 ± 0.3 pS (mean ± S.D.).

The amplitude histogram also shows the existence of a subconductance state which is characterized by the value: 2.37 ± 0.57 pS (mean ± S.D., $n = 293$). The presence of the subconductances events is observed, specially at high potential, in Fig. 3.3.

Other conductances were found in few experiments. The presence of conductances around 7 pS and 50 pS was observed. Fig. 3.6 and 3.7 show these recordings.

When the concentration less than 3 μM, no channel activation can be observed in our experiments. In the experiments, domoic acid concentration was 10 μM. No obvious desensitization was observed with this concentration. We have not done systematical experiments to test the effects of higher concentration of domoic acid.

Time Distribution

A typical dwell-time histogram is shown in Fig. 3.8. The opening state histogram has one peak at $\tau_o = 2.91 \pm 1.25$ ms (mean±S.D. $n = 3$). However, the closing state histogram has two peaks, one locates

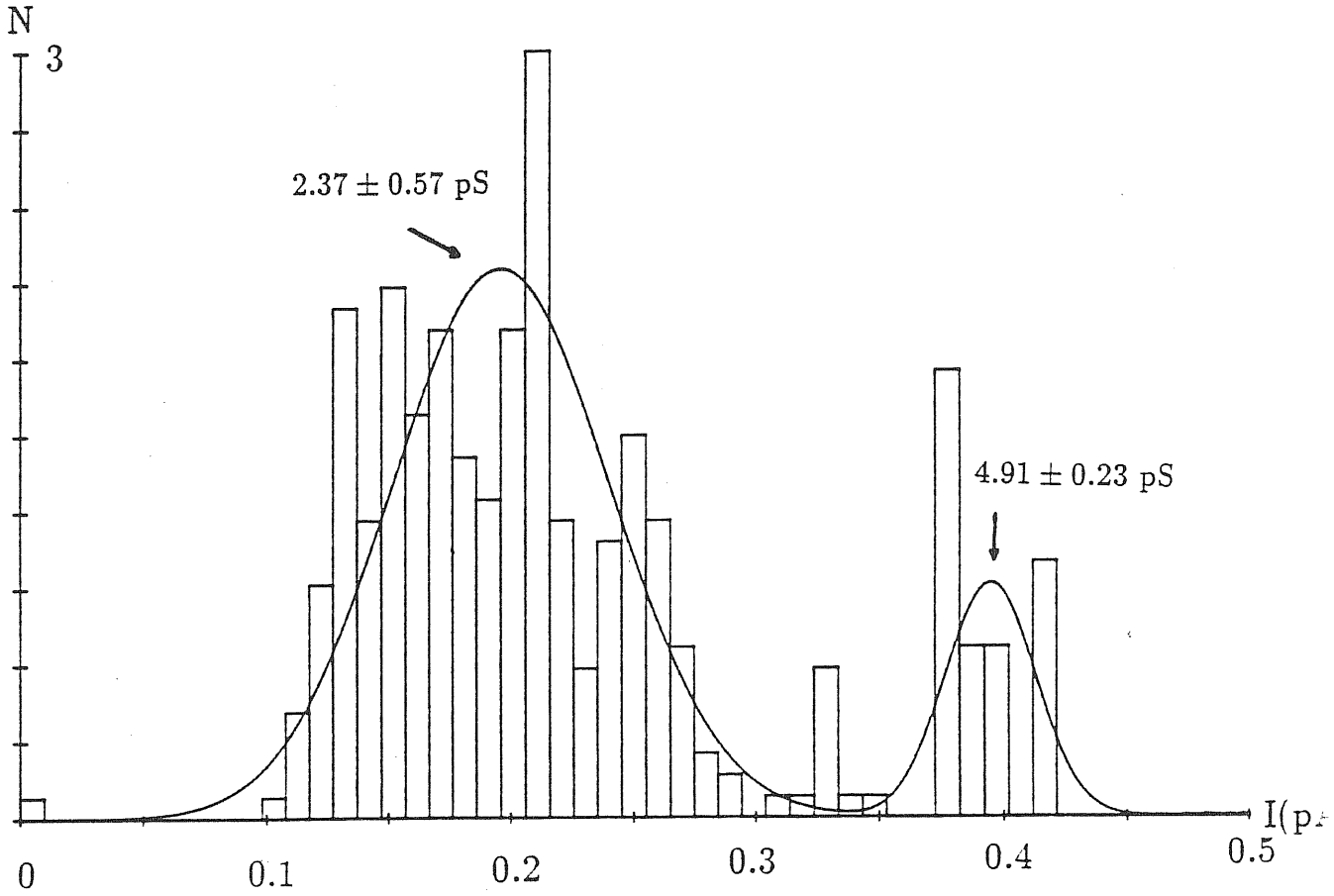

Fig. 3.5 Current amplitude histogram of outside-out patches obtained from granule cells of 8 days *in vitro*. Membrane potential was −80 mV. Temperature was 24°C. Filter was 500 Hz. The bin was 0.01 pA wide and the event number was 344. The histogram was fitted with Gaussian function and shows two peaks locating at 0.19 ± 0.57 and 0.39 ± 0.23 pA respectively. Conductance values are indicated in the figure.

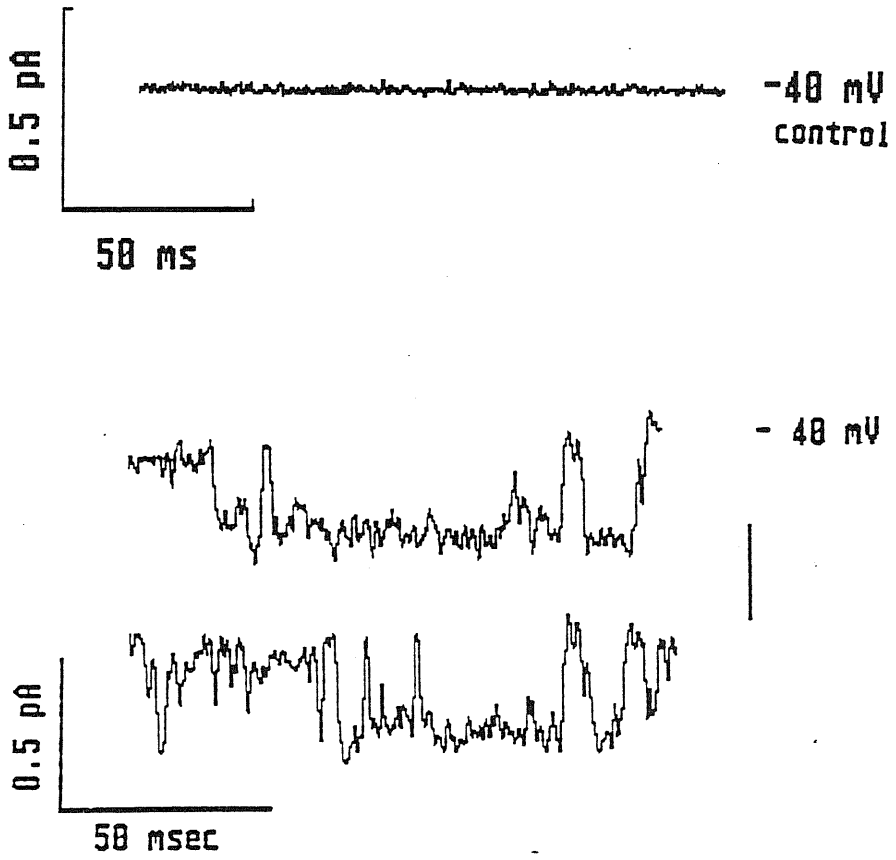

Fig 3.6 A conductance about 7 pS was observed in cell-attached patches. Obtained from granule cells of 8 days *in vitro*.Temperature was 21°C. Electrode potential varied from −40 mV to 40 mV, corresponding a membrane potential range from −110 mV to −30 mV. 10μM domoic acid was applied in pipette solution.

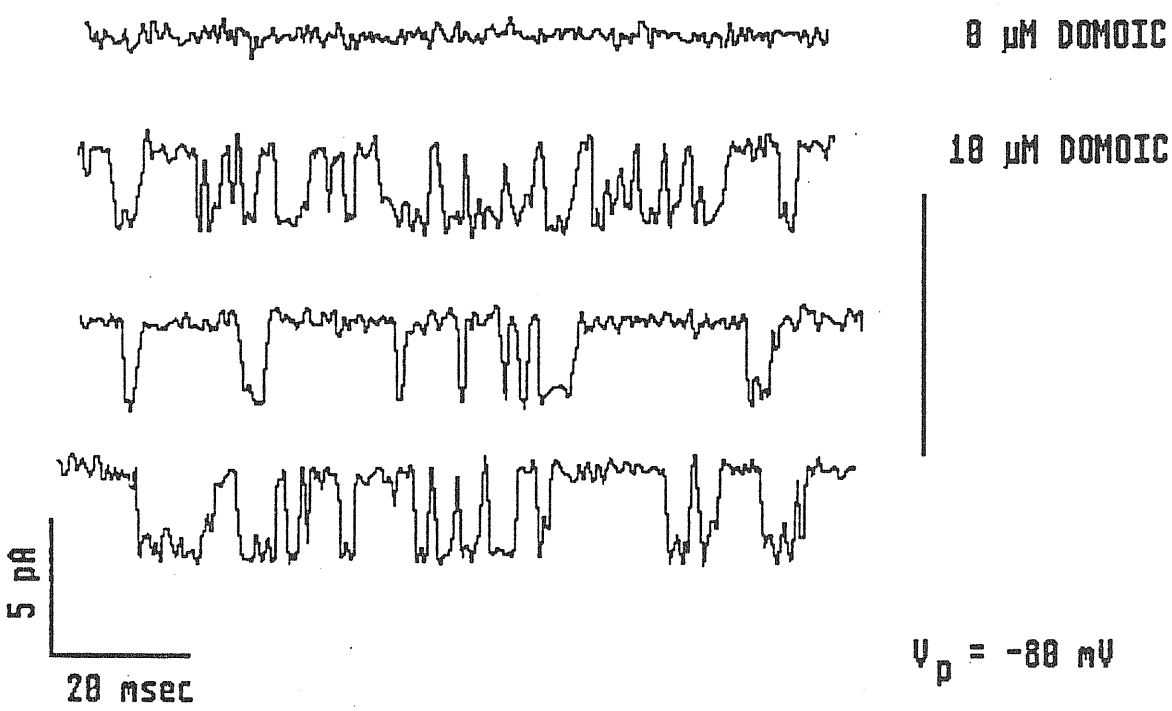

Fig 3.7 A conductance about 50 pS was observed in outside-out patch. Obtained from granule cells of 5 days *in vitro*. Temperature was 19°C. Membrane potential was −80 mV. 10μM domoic acid was applied in bath solution.

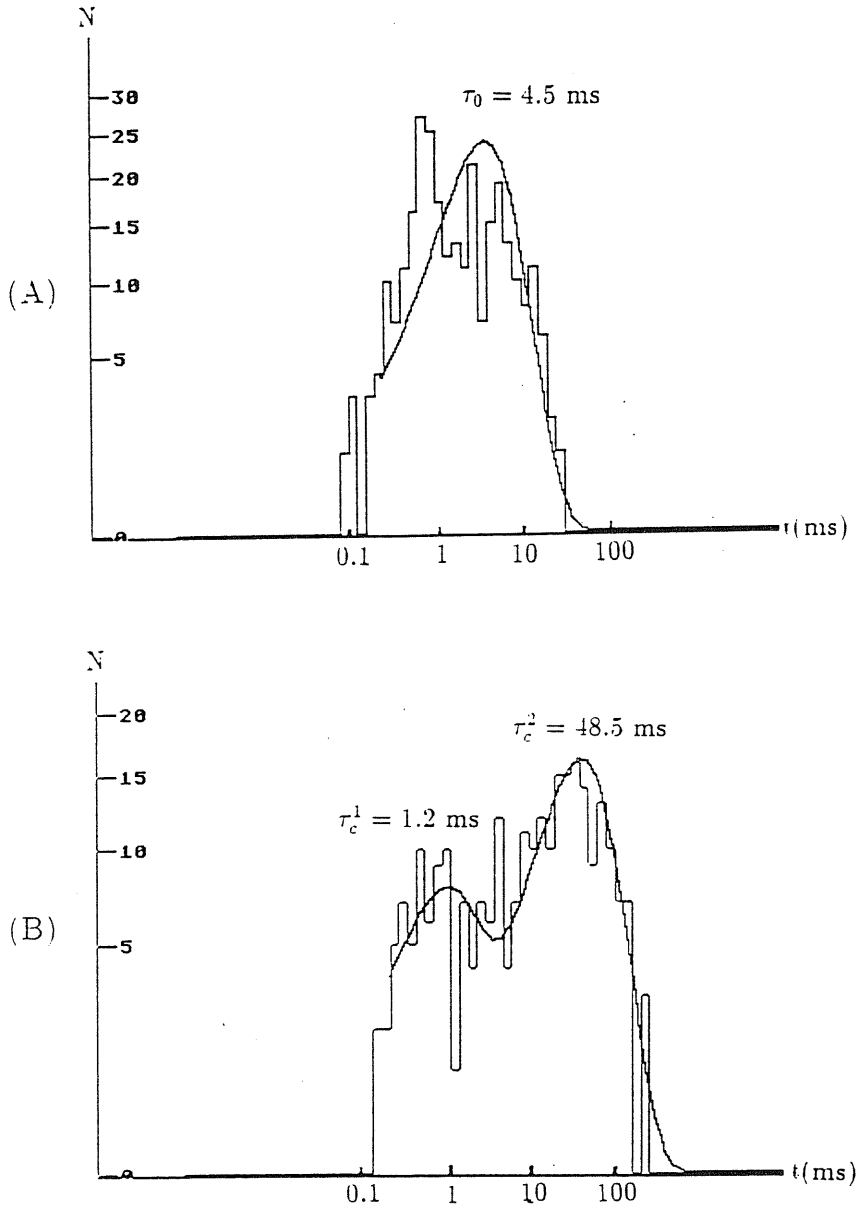

Fig 3.8 Dwell-time distribution histogram of domoic activated channels. Obtained from outside-out experiments. The granule cells are 8 days *in vitro*. Temperature was 24°C. Membrane potential was −80 mV. Bandwidth was 500 Hz. The bin was 0.1 wide in logarithmic scale. The histograms were fitted with the sum of the exponential function: $a_i e^{-t/\tau_i}$. The number of events was 272. (A) histogram of open state dwell-time. (B) histogram of closed state dwell-time.

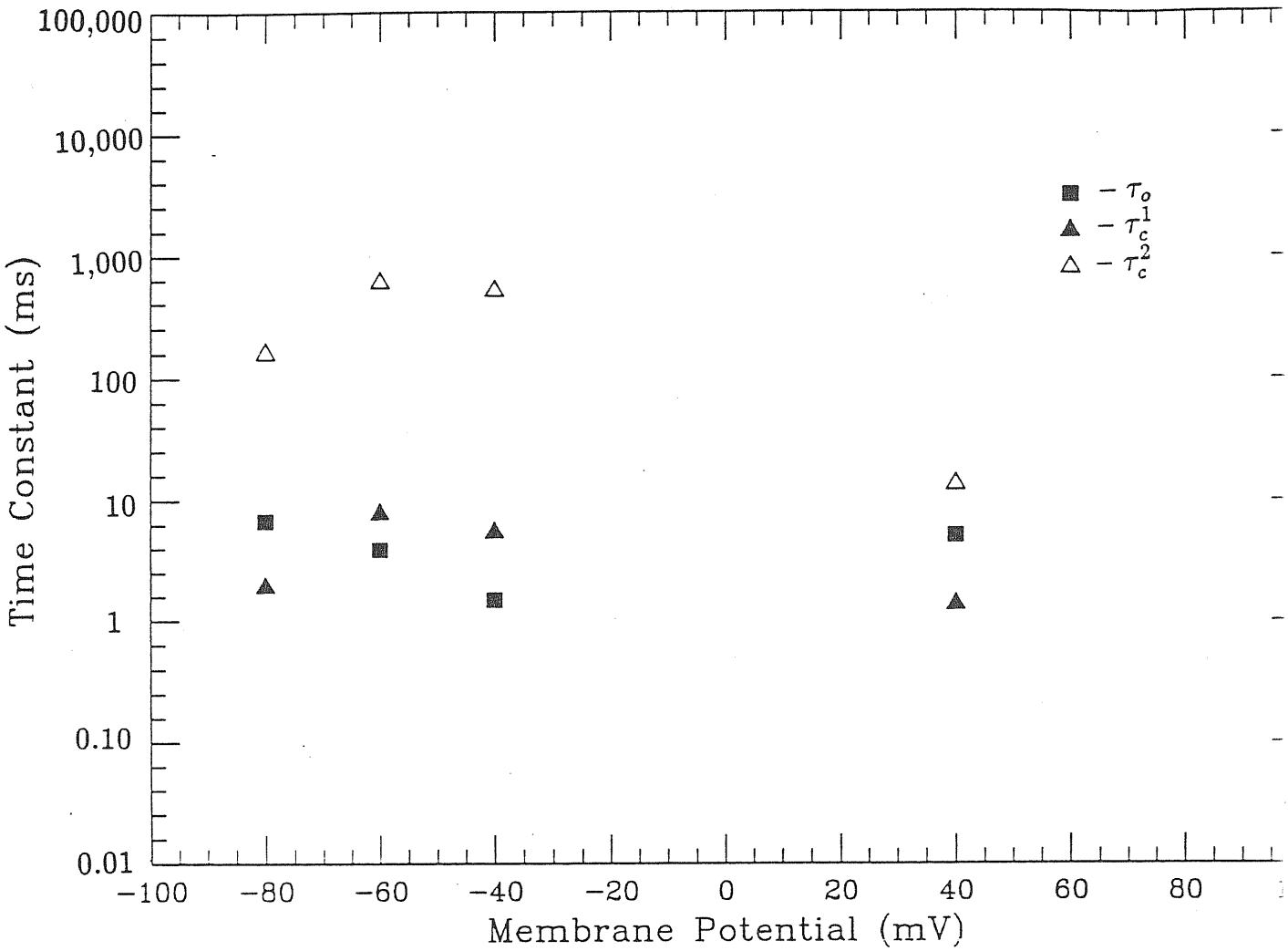

Fig. 3.9 Time constants distribution at different membrane potentials. The values in this graph are the average of three experiments.

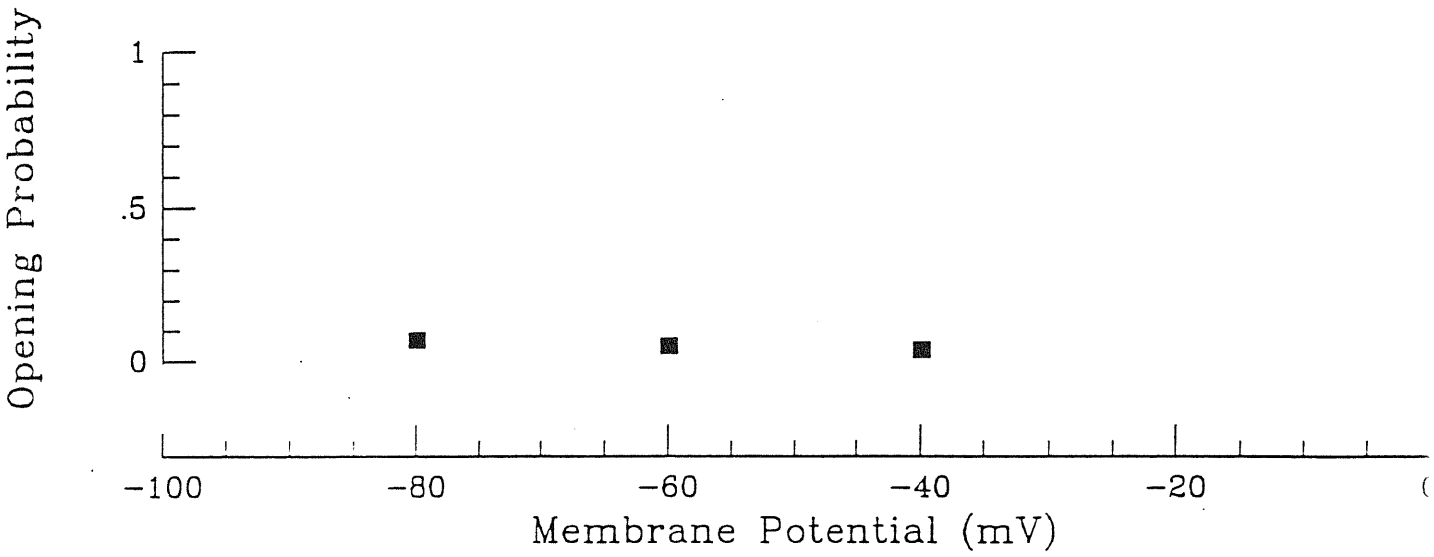

Fig. 3.10 The opening probabilities at different membrane potentials.

at $\tau_c^1 = 1.27 \pm 0.27$ ms (mean±S.D. $n = 3$) and the other locates at $\tau_c^2 =$ 110±47 ms (mean±S.D. $n = 3$). This histogram indicates that the channels, activated by domoic acid, have one opening state and two closing states.

Theoretically, mean opening time $< t_o >$ should be equal to the dwell-time τ_o of opening state if the histogram can be fitted with a single exponential function. Comparing the value of 3.03 ± 1.25 ms (mean±S.D. $n = 3$)obtained for $< t_o >$ with the above mentioned τ_o that demonstrates there exists exactly only one peak in opening state dwell-time histogram.

In Fig. 3.9, the relationship of time constant, τ_o, τ_c^1 and τ_c^2, and membrane potential is shown. Membrane potential has no obvious influence on the time constant fluctuations.

The influence of membrane potential on the opening probability is shown in Fig. 3.10. It seems that the fluctuation of the opening probability does not depend on the membrane potential because there is no obvious relation can be found between this two quantities. But in any case these data are too few to allow a firm conclusion.

Chapter 4

Discussion

Conductances

Jahr and Stevens (1987) reported that at least five distinct current levels could be induced by glutamate through the three subtypes of excitatory amino acid receptors. Fig. 4.1 displays sample records obtained with prolonged application of 10 μM glutamate. The conductance events can be divided into three categories: small (5 $\sim$ 15 pS), medium (20 $\sim$ 35 pS) and large (40 $\sim$ 50 pS). Small and large events are common but the medium-size are relatively infrequent.

The selective glutamate agonists, NMDA, kainate and quisqualate, preferentially activate subpopulations of the conductances. Although all three agonists do produce some openings of all three sizes, NMDA tends to cause large openings. Kainate usually produces events of conductance $\leq$5 pS whereas quisqualate activates 10 pS and 15 pS events more than kainate (Jahr and Stevens 1987).

In our experiments, both outside-out and cell-attached recordings show a main event with conductance about 4 pS and mean open time less than 4 ms. This characteristic coincides with the kainate-induced currents

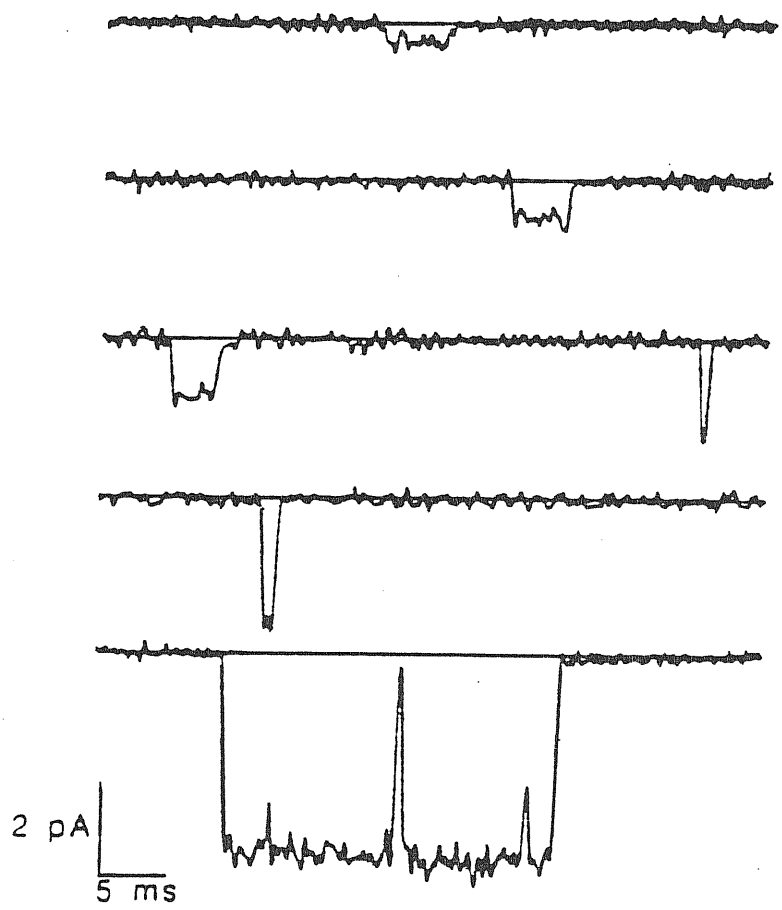

Fig. 4.1 Outside-out recordings shows at least 5 distinct conductance events caused by 10 μM glutamate at -80 mV. (from Jahr and Stevens 1987)

described by Ascher and Nowak (1988), using outside-out record in combination with spectral analysis and variance analysis. Comparing our results with those of Jahr and Stevens (1987), Cull-Candy and Usowicz (1987) and Ascher and Nowak (1988), we can deduce reasonably that domoic acid acts preferentially on the kainate receptors of the cell membrane. This consequence coincides with the conclusion that domoic acid has a high affinity for the kainate receptors (Slevin, *et al.* 1983, Hampson and Wenthold 1988).

Some of our cell-attached recordings show the presence of an event with conductance around 7 pS and the similar opening time as the main component (see Fig.3.6). Although this 7 pS event seems like the double events of 4 pS or the summation of the main conductance and the sub-conductance, in fact it is not. The pipettes used in our experiments had a unsealed resistance about 10 MΩ, the areas of the tip opening according to the empirical experiences (Sakmann and Neher 1983) were less than 5μm^2. Patlak and his colleagues (1979) illustrated that the frequency of the simultaneous opening of two or more channels in these small patches is very low or zero. So it is impossible to assume two independent channels will open always together to form a current trace as Fig.3.6 shows. Maybe this 7 pS component the one usually is caused by quisqualate, but the evidences are too few to allow a firm conclusion.

The 50 pS event appeared in outside-out recording has the same properties as the main component of NMDA-induced current. This phenomena is the same as Cull-Candy and Usowicz described (1987) when they studied kainate activated channels. They found the high concentrated kainate (50μM) can also activate the largest current produced by glutamate, although at normal concentration it usually open only the small conduc-

tance channels. In our experiments, the domoic acid was directly applied in bath solution using pipette. The concentration of domoic acid was calculated on the basis that the volume of the bath solution was 2 ml. Therefore, in practice the domoic concentration will fluctuate slightly depending on the error of the bath solution volume. May be in that experiment, from which we found the 50 pS conductance, the domoic concentration was more than 10 μM because of the less volume of the bath solution. Of course, the domoic acid concentration will not reach as high as 50μM causing by fluctuation but only around 10μM. But if we remind that the domoic acid is equal or more potent than kainate (Biscoe *et al.*, 1975), may be this higher concentration can also activate the large conductance channels.

Ionic Selectivity

It is already known that glutamate analogues activated channels are permeable mainly to monovalent cations (MacDonald and Wojtowicz 1980, Crunelli *et al.*, 1984, Hablitz and Langmoen 1983), and some of them can also activate a conductance that permits significant calcium influx (Ascher and Nowak 1986, MacDermott *et al.*, 1986). Therefore, in below discussion we only talk about monovalent cations. The fact that domoic acid elicited current invert at 0 mV indicates that the channels activated by domoic acid are equally permeable to cations. From Goldman-Hodgkin-Katz constant-field theory (Goldman 1943, Hodgkin and Katz 1949), the reversal potential in our experimental condition is determined by the equation:

$$E_{rev} = \frac{RT}{F} ln \frac{P_K[K^+]_o + P_{Na}[Na^+]_o + P_{Cs}[Cs^+]_o}{P_K[K^+]_i + P_{Na}[Na^+]_i + P_{Cs}[Cs^+]_i} \qquad (4.1)$$

where P expresses the permeability of each ion and $[\ ]_i$, $[\ ]_o$ express the concentrations of each ion inside and outside the membrane respectively. In standard condition (see table 2.7 and 2.8):

$$[Na^+]_o + [K^+]_o + [Cs^+]_o = [Na^+]_i + [K^+]_i + [Cs^+]_i \tag{4.2}$$

In order to let Eq(4.1) equal to zero under the condition (4.2), we should assume:

$$P_{Na} = P_K = P_{Cs} \tag{4.3}$$

That says: domoic acid activated channels permeate equally to Na^+, K^+ and Cs^+.

Voltage Dependence

In our results, the dwell-times and opening probability are roughly the same at different membrane potentials (see Fig. 3.9 and 3.10). In other words, the kinetic process of domoic acid activated channels are not voltage dependent. This property suggests that the sensor of the channels responds only to the ligand-binding of neurotransmitter, but not to the voltage field. That demonstrates the domoic activated channels are neurotransmitter gated channels without voltage dependence.

Slightly differences in the single channel conductances have been observed at different applied potentials. This rectification in $I - V$ relations

indicates that the membrane potential has some influences on the conductance of domoic-activated channels. Ascher and Nowak (1988) have reported Similar effects about KA activated channels, that should be the same receptor-channel complex as that is activated by domoic acid. This phenomena can be due to the different mobilities of the ions in each side of the membrane. According to this idea, the rectification will be influenced by the ionic concentration combinations in the internal and external side of the membrane. Therefore, further studies have to be done to investigate this point.

Neurotoxicity

Neurotoxicity measurement has been a method to evaluate the neurotransmitter. The neurotoxicity is widely studied using the cells in culture (for example see Novelli *et al.*, 1988, McCaslin and Smith 1988). The effects of EAA neurotoxicity on the cells has been proposed in terms of the depolarization of cells and the Ca^{2+} entering the cells.

However, it is necessary to observed that the EAA neurotoxicity at systemic level can be due to the cell connection interferences. If certain quantity of EAA, that is not enough to produce cellular neurotoxicity, is applied to the neuron tissue, it can "short circuit" the normal cell to cell communication flux, and introduce important disorders that will be reflected as neurological symptoms.

On the bases of our results, we can estimate the toxicity of domoic acid. The diameter of granule cells' body is $5 \sim 10\mu$m. Its surface area can be roughly estimated as $314\mu m^2$. We also have an estimation about

the channel density, opening probability and single channel conductance. Thus, we can see what should happen with the current that domoic acid activated channels introduce. We simulated the effects of the domoic acid evoked current in an excitable cell using the Hodgkin and Huxley (1952) model in a program (Moran *et al.*, 1986), in which this EAA current was introduced.

Three experimental conditions were simulated: first, 10μM domoic acid application; second, 10 times effective domoic acid application; third, 50 times effective domoic acid application. We must emphasize here that it is just the effect but not the concentration which has been amplified.

From Fig 4.2 we can see that 10μM domoic acid did not maintain depolarization of the cell but it produced a repetitive firing. Since the cells continue to fire, the sodium will accumulate in the cells and the potassium will be lost. If the firing is continuous, the amount of energy required to activate the Na-K pump will not be sufficient to recover the cells back to the normal state, thus the cells will die. If the effect of domoic acid is increased to 50 times of that of 10 μM domoic acid, the cells will keep in depolarization state and the cells have no response to other stimulus. In this case, a lack of strong energy sources will also produce the cell death. Supposing this mechanism is correct, the main problem will be the lack of energy compensation.

Novelli and his colleagues (1988) reported some interesting results that are in line with this hypothesis. They found that the absence of glucose in the medium increase the neurotoxicity of EAA. They also reported that the neurotoxicity could be increased by the adding of KCN or Ouabain to

the medium. From their results it is possible to conclude that the energy requirements of the cell, and specially the activating of the Na-K ATPase, is involved in the neurotoxic mechanism of the EAA.

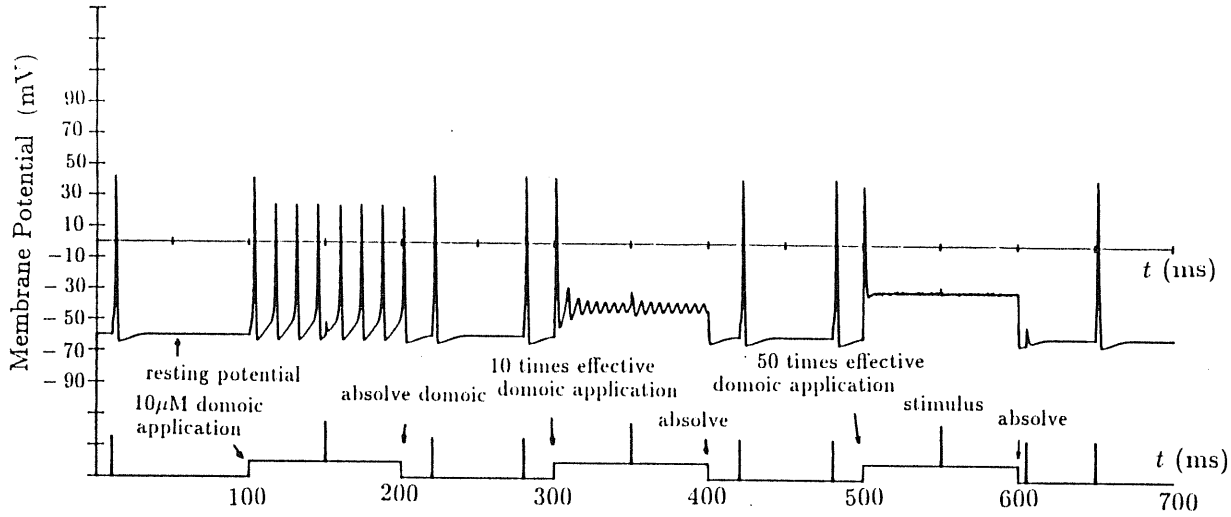

Fig. 4.2 Computer simulation of the effects of domoic acid on granule cells. The lower trace gave the simulate conditions: the peaks correspond the stimulus; domoic acid was applied in extracellular solution during the time intervals $100 \sim 200$ ms, $300 \sim 400$ ms and $500 \sim 600$ ms; the effects were 1, 10 times and 50 times in order.

Conclusions

1. The result presented here shows that domoic acid activates mainly the channels with conductance around 4 pS and mean open time about 3 ms. It can also activated channels with other conductances. In our experiments, we found another two conductances: one is about 7 pS and another one is about 50 pS. They are possible related to a non-specific activation of other glutamate receptors.

2. This channel characteristics are consistent with the hypothesis that domoic acid is an agonist of the KA receptor, one of the glutamate receptor subtypes.

3. When domoic acid molecules bind on the KA receptors, they open the channels to allow monovalent cations to permeate equally. This function lead the reversal potential of domoic acid activated channels is 0 mV when the monovalent cations concentrations of solution in the pipette and in the bath are equal.

4. The kinetic of the domoic acid activated channels can be described as one open state and two closed states. The dwell-times and opening probability are independent to the membrane potentials.

Acknowledgements

I would like to express my gratitudes to my professor Antonio Borsellino, who guided me to study and gave me continuous support during these two years. The gratitudes also for his carefully correction and powerful pushing of my thesis. I greatly appreciate professor Oscar Moran for his helpful instruction during the whole process of my work in the Biophysics Laboratory of SISSA and for his kindly correction and improvement of my thesis. The appreciation should go to Dr. Marina Sciancalepore, who made important contributions to my work. Here I want to express my thanks to all the members in the Biophysics Laboratory of SISSA. I would also like to express my thanks to Dr. Antonello Novelli for his very important information and kindly providing references. Thanks are also due to Dr. Walter Stühmer from Max-Planck institut für biophysikalische Chemie, Göttingen, FRG.for the AD-DA convertor prototypes and H. Affolter from Instrutek (NY. USA.) and Yale University for the software. I also acknowledge Dr. Lin Fan and Dr. Gilberto Giugliarelli for their helping in using computer. Mrs. Judy Geiger help me to improve the English through all the thesis, I want to express my gratitudes to her for the warm helps. The Department of BBCM of Trieste University is also acknowledged for the providing of rats. At last, L should express my thanks to Dr. Zhang Ling for here very kindly and warmly help in typing this thesis.

References

[1] Alberts, B., Bray, D., Lewis, J., Raff, M., Roberts, K. & Watson, J. D. (1983) *Molecular Biology of the cell.* Gerland publishing, Inc. New York, U.S.A.

[2] Ascher, P. & Nowak, L. (1986) *J. Physiol. Lond.* **377**, 43

[3] Ascher, P. & Nowak, L. (1988) *J. Physiol. Lond.* **399**, 227

[4] Bernstein, J. (1902) *Pflügers Arch.* **82**,521

[5] Bernstein,J. (1912) *Elektrobiologie* Viewag, Braunschweig

[6] Biscoe, T. J., Duggan, A.W., & Lodge, D. (1972) *Comp. Gen. Pharmac.* **3**, 423

[7] Biscoe, T. J., Evans, R. H., Headley, P. M., Martin, M. & Watkins, J. C. (1975) *Nature* **255**, 166

[8] Borsellino, A., Galdzicki, Z., Novelli, A., Puia, G. & Sciancalepore, M. (1988) *11th Annual meeting of the European Neuroscience Association, Eur. J. Neurosci. suppl.* **42**

[9] Braitenberg, V. & Atwood, R. P. (1958) *J. Comp. Neurol.* **109**, 1

[10] Castillo, J. del & Stark, L. (1952) *J. Physiol.* **116**,507

[11] Chiara, G. di & Gessa, G. L. (1981) *Adv. Biochem. Psychopharm.* **27**

[12] Cole, K. S. (1949) *Arch. Sci. Physiol.* **3**, 253

[13] Colquhoun, D. & Sigworth, F. J. (1983) Fitting and statistical analysis of single-channel records. In: *Single channel recording.* Sakmann, B. and Neher, E. (Eds.) Plenum Press, New York

[14] Crunelli, V., Forda, S. & Kelly, J. S. (1984) *J. Physiol. Lond.* **351**, 327

[15] Cull-Candy, S. G. & Ogden, D. C. (1986) *Ion channels in Neural Membranes.* Alan R. Liss, Inc., New York

[16] Cull-Candy, S. G. & Usowicz, M. M. (1987) *Nature* **325**, 525

[17] Cull-Candy, S. G., Howe, J. R. & Ogden, D. C. (1988) Noise and single channels activated by excitatory amino acids in rat cerebellar granule neurones. *J. Physiol. Lond.* **400**,

[18] Curtis, D. R. & Johnston, G. A. R. (1974) *Ergebn. Physio.* **69**, 97

[19] Curtis, D. R., Phillis, J. W. & Watkins, J. C. (1959) *Nature* **183**, 611

[20] Curtis, D. R., Phillis, J. W. & Watkins, J. C. (1960) *J. Physiol. Lond.* **150**, 656

[21] Curtis, D. R., Watkins, J. C. (1960) *J. Neurochem.* **6**, 117

[22] Curtis, D. R., Watkins, J. C. (1963) *J. Physiol.* **166**, 1

[23] Dale, H. H. (1953) *Adventures in physiology.* Pergamon Press, London

[24] Davies, J. D. & Watkins, J. C. (1977) *Brain Res.* **130**, 364

[25] Douglas, W. W. (1978) *Ciba Fdn. symp.* **54**, 61

[26] Duggan, A. W. (1974) *Expl. Brain Res.* **19**, 522

[27] Evans, R. H., Francis, A. A. & Watkins, J. C. (1977) *Experientia* **33**,489

[28] Foster, A. C. & Fagg, G. E. (1984) *Brain Res. Rev.* **7**, 103

[29] Gallo, V., Ciotti, M. T., Coletti, A., Aloisi, F. & Levi, G. (1982) *Proc. Natl. Acad. Sci. USA.* **79**, 220

[30] Hablitz, J. J. & Langmoen, I. A. (1982) *J. Physiol. Lond.* **325**,317

[31] Hamill, O. P., Marty, A., Neher, E., Sakmann, B. & Sigworth, F. J. (1981) *Pflügers Arch.* **391**, 85

[32] Hamill, O. P. & Sakmann, B, (1981) *J. Physiol. Lond.* **312**, 41

[33] Hampson, D. R. & Wenthold, R. J. (1988) *The J. of Biol. Chem.* **263**, No. 5, 2500

[34] Hille, B. (1984) *Ionic channels of excitable membranes.* Sinauer Associates, Inc., Sunderland

[35] Hockberger, P. E., Tseng, H. & Connor, J. A. (1987) *The J. of Neurosci.* **7**, 1370

[37] Hodgkin, A. L. & Huxley, A. F. (1952) *J. Physiol. Lond.* **117**, 500

[38] Horn, R. & Patlak, J. B. (1980) *Proc. Natl. Acad. Sci. USA.* **77**, 6930

[39] Iversen L. L. (1984) *Proc. R. Soc. Lond.* **B221**, 245

[40] Jahr, C. E. & Stevens, C. F. (1987) *Nature* **325**,522

[41] Johnston, G. A. R., Curtis, D. R., Davies, J., & McCulloch, R. M. (1974) *Nature* **248**, 804

[42] Kohler, C. & Schuarcz, R. (1983) *Neuroscience* **8**, 819

[43] Kolb, B. & Whishaw, I. Q. (1980) *Fundamentals of human neuropsychology.* W.H.Rreeman and Company, New York

[44] Krnjević, K. (1974) *Physiol. Rev.* **54**, 418

[45] Krnjević, K. & Phillis, J. W. (1963) *J. Physiol. Lond.* **165**, 274

[46] Kuffler, S. W., Nicholls, J. G. & Martin, A. R. (1984) *From neuron to brain: a cellular approach to the function of the nervous system.* Sinauer Associates Inc., Sunderland

[47] Lakshminarayanaiah, N. (1984) *Equations of membrane biophysics.* Chapter 7, Academic Press Inc., London

[48] Langley, J. N. & Anderson, H. K. (1892) *J. Physiol.* **13**, 460

[49] Läuger, P. (1975) *Biochem. Biophys. Acta.* **413**, 1,

[50] Lin, F. & Moran, O. (1988) *12th Annual meeting of the European Neuroscience Association Suppl. 2*, abs. no. 44.11

[51] Lin, F. (1988) Sodium current on rat cerebellar granule cells. *Magister thesis*

[52] Loewi, O. (1921) *Pflügers Arch.* **189**, 239

[53] MacDermott, A. B., Mayer, M. L., Westbrook, G. L., Smith, S. J. & Barker, J. L. (1986) *Nature* **321**, 519

[54] MacDonald, J. F. & Wajtowicz, J. M. (1980) *Can. J. Physiol. Pharmac.* **58**, 1393

[55] Marmont, G. (1949) *J. Cell. Comp. Physiol.* **34**, 351

[56] Mayer, M. L. & Westbrook, G. L. (1987) *Prog. in Neurobiol.* **28**, 197

[57] McCaslin, P. P. & Smith, T. G. (1988) *Europ. J. Pharmacol.* **152**, 341

[58] McCulloch, R. M., Johnston, G. A. R., Game, C. J. A. & Curtis, D. R. (1974) *Expl. Brain Res.* **21**, 515

[59] McGeer, E. G., Olney, J. W. & McGeer, P. L. (Eds.) (1978) *Kainic acid as a tool in Neurobiology.* Raven Press, New York

[60] McLennan, H. (1981) *Glutamate as a Neurotransmitter.* Raven Press, New york

[61] McLennan, H. (1987) Setting the scene: The Excitatory Amino Acids—30 years on. In: *Excitatory Amino Acid Transmission* Hicks, T. P., Lodge, D. & McLennan, H. (Eds.), Alan R. Liss, Inc., New York

[62] Moran, O., Smith, J. E. *Y* Requena, J. (1986) *Interciencia.* **11**, No. 2,

[63] Neher, E. (1981) Unit conductance studies in biological membranes. In: *Techniques in cellular physiology.* Baker, P. F. (Ed.), Elsevier/NorthHolland, Amsterdam

[64] Neher, E. & Sakmann, B. (1976) *Nature* **260**, 799

[65] Nernst, W. (1888) Zur kinetik der iösung befindlichen körper: theorie der diffusion. *Z. Phys. Chem.* 613

[66] Novelli, A., Reilly, J. A., Lysko, P. G. & Henneberry, R. C. (1988) *Brain Res.* **451**, 205

[67] Patlak, J. B., Gration, K. A. F. & Usherwood, P. N. R. (1979) *Nature* **278**, 643

[68] Sayan, O. R. (1987) Primary neuron culture: isolation of glutamatergic cerebellar granule cell from eight day old sprague dawley rat. *Internal report from National Institutes of Health, U.S.A.*

[69] Sciancalepore, M. & Moran, O. (1988) *12th Annual meeting of the European Neuroscience Association Suppl. 2*, abs. no. 44.10

[70] Shannon, C. E. & Weaver, W. (1964) *The mathematical theory of communication.* The University of Illinois Press, Urbana

[71] Shinozaki, H. (1978) Discovery of novel actions of kainic acid and related compounds. In: *Kainic acid as a tool in neurobiology.* McGeer, E. G., Olney, J. M. & McGeer, P. L. (Eds.), Raven Press, New York

[72] Shinozaki, H. (1988) *Prog. in Neurobiol.* **30**, 399

[73] Shinozaki, H. & Konishi, S. (1970) *Brain Res.* **24**, 368

[74] Shinozaki, H. & Shibuya, I. (1974) *Neuropharmacol.* **13**, 665

[75] Shinozaki, H. & Shibuya, I. (1976) *Neuropharmacol.* **15**, 145

[76] Sigworth, F. J. & Sine, S. M. (1987) *Biophys. J.* **52**, 1047,

[77] Slevin, J. T., Collins, J. F., Lindsley, K. & Coyle, J. T. (1983) *Brain Res.* **265**, 169

[78] Stevens, C. F. (1972) *Biophys. J.* **12**,1028

[79] Usowicz, M. M., Gallo, V. & Cull-Candy, S. G. (1989) *Nature* **339**, 380

[80] Watkins, J. C. & Evans, R. H. (1981) *Annu. Rev. Pharmacol. Toxicol.* **21**, 165